DOI: 10.1002/chem.200801394

Synthesis and Conformational Analysis of (α-D-Galactosyl)phenylmethane and α-,β-Difluoromethane Analogues: Interactions with the Plant Lectin Viscumin

Maria Kolympadi,[a] Marco Fontanella,[b] Chiara Venturi,[b] Sabine André,[c] Hans-Joachim Gabius,[c] Jesús Jiménez-Barbero,*[b] and Pierre Vogel*[a]

Abstract: (α-D-Galactosyl)phenylmethane (**1**), (α- and β-D-galactosyl)-(difluoro)phenylmethane (**2** and **3**) have been prepared and their conformations in solution were described by using a combination of force-field calculations and NMR spectroscopic studies. Galactoside **1** adopts a $^4C_1$ chair conformation and an *exo* anomeric orientation, as is the case for natural α-galactosides. The X-ray crystal structure of its difluoromethylene derivative **2** similarly shows a $^4C_1$ chair conformation. Surprisingly, compound **2** exhibits a different equilibrium between $^1C_4$ chair and $^1S_3$ skew boat conformations and significant flexibility around the pseudoglycosidic linkage when in solution. The β-stereoisomer **3** adopts a major $^4C_1$ chair conformation. Interestingly, *C*-galactosides **1**, **2**, and **3** bind to viscumin (VAA), a galactoside-specific lectin, which is confirmed by NMR experiments and docking calculations.

Keywords: carbohydrate mimics · lectin · molecular modeling · NMR spectroscopy · protein structures

Introduction

Recognition processes involving carbohydrate moieties of cellular glycoconjugates have a significant impact on different aspects of cell biology as they are involved in mediating communication between cells and their environment.[1] Decoding of the glycan signals is performed by lectins (carbohydrate-binding proteins without enzymatic activity, excluding antibodies and transport proteins for free glycans).[1,2] The protein superfamily, by virtue of its effector functionality, is thus becoming an attractive target for drug design, for example, to block harmful effects of pro-inflammatory mediators or interfere with cell binding of toxic lectins. In the latter case, viscumin, also referred to as *Viscum album* agglutinin (VAA), is a potent biohazard akin to ricin, whose toxicity can be neutralized by suitable inhibitors competing with the cell-surface glycans.[3] This has made the toxin a model for drug design, for example, applying library approaches in search of new binding partners.[4] On a broad scale, the study of potent lectin counter-receptors will not only provide a source for new pharmaceuticals, but also valuable insights into the mechanisms of protein–carbohydrate interactions.[2b,5]

Carbohydrate mimics such as *C*-glycosides[6] in which the anomeric oxygen has been replaced by a methylene or a substituted methylene unit, exhibit stability against chemical and enzymatic hydrolysis and, depending on substitution, improved pharmacokinetic properties over the natural saccharides. Beyond these advantages, of concern is whether these pseudosaccharides maintain an affinity towards the same receptors, taking into account that such an alteration of the glycosidic bond can lead to conformational changes of the intersaccharide torsions and may also affect the saccharide ring. As we previously reported,[7] *C*-analogues are more flexible, possibly owing to the absence of the *exo*-

[a] M. Kolympadi, Prof. Dr. P. Vogel
Laboratoire de Glycochimie et Synthèse Asymétrique (LGSA)
Swiss Federal Institute of Technology (EPFL)
Batochime, 1015 Lausanne (Switzerland)
Fax: (+41) 216-939-375
E-mail: pierre.vogel@epfl.ch

[b] Dr. M. Fontanella, Dr. C. Venturi, Prof. Dr. J. Jiménez-Barbero
Centro de Investigaciones Biológicas, CSIC
Ramiro de Maeztu 9, 28040 Madrid (Spain)
Fax: (+34) 915-360-432
E-mail: jjbarbero@cib.csic.es

[c] Priv.-Doz. Dr. S. André, Prof. Dr. H.-J. Gabius
Institute of Physiological Chemistry
Faculty of Veterinary Medicine, Ludwig-Maximilians-University
Veterinärstrasse 13, 80539 Munich (Germany)

Supporting information for this article is available on the WWW under http://dx.doi.org/10.1002/chem.200801394.

anomeric effect, and show a distribution of different conformers. Nevertheless, if the energy barriers between these conformers are small, a global-minimum-bound conformation with the receptor protein might be achieved, thus exceeding the entropic penalty.[2b,8] Whilst in cases where the bound conformation resembles the ground state of *O*-glycosides, *C*-glycosides with closer conformation behavior to *O*-glycosides would be desirable.[9]

Introduction of fluorine atoms at the pseudoanomeric center of a *C*-saccharide can "correct" the polarity of this position relative to the native glycosidic oxygen and increase the lipophilicity of the entire molecule.[10] As a matter of fact, CF_2 and CHF groups have been examined as isosteres of oxygen in biologically active compounds[11] and the *gauche* conformation of 2-fluoroethanol and related structures is well documented.[12] In the course of our search for sugar mimics, we are interested in the preparation of CF_2-galactopyranosides, and the exploration of their conformation profile. Synthetic methods towards CF_2-furanosides[13] and pyranosides[14] have been described by different research groups. We have reported the preparation of a CHF-disaccharide of glucose whose study in solution revealed unusual conformations to exist in equilibrium with "normal" conformations for *C*-glycosides.[14b] Mootoo and co-workers developed a *de novo* synthesis of β-CF_2- and β-CHF-galactopyranosides,[14h] thus preparing three fluorinated *C*-disaccharides. These mimics of sialyl Le^X and their conformation in solution, along with their activity towards the C-type lectin P-selectin involved in inflammation were investigated.[14i,15] Moreover, biologically useful pseudoglycopeptides of CF_2-galactopyranosylesters were reported by Leclerc, Quirion, and co-workers,[14a,c,f,g,k] as well as CF_2-sialylgalactose by Sodeoka and co-workers.[14j]

Herein, we present the synthesis and the conformational analysis of three simple phenyl *C*-galactopyranosides: (α-D-galactosyl)phenylmethane **1**, (α- and β-D-galactosyl)-(difluoro)phenylmethane **2** and **3**, respectively. Syntheses of the glucose and mannose series of **1** are already known.[16] To the best of our knowledge, **2** is the first example of α-CF_2-galactosides,[17] however, a protected form of **3** was also recently described.[14h] We performed a conformational analysis of these molecules by using a combination of molecular dynamics and NMR spectroscopy and have shown that chemical changes at the pseudoanomeric center have important effects on the behavior of these *C*-galactosides in solution. To study their capacity as bioactive ligands, interactions of **1**, **2**, and **3** with the galactoside-binding VAA lectin, which has two combining sites and is active with α and β anomers,[18] were monitored by NMR experiments and docking calculations.

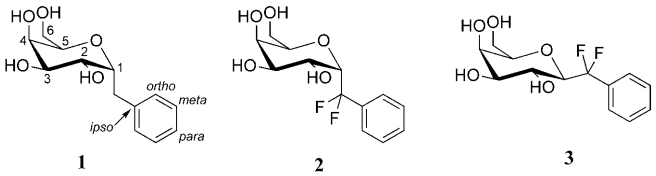

1 **2** **3**

Results and Discussion

Synthesis: Key intermediates in the parallel synthesis of **1**, **2**, and **3** are the α- and β-D-*C*-galactosyl carbaldehydes **7** and **8**, respectively,[19] which were prepared by using a modified sequence described by Bednarski and co-workers[19a] (Scheme 1). Reaction of galactose pentaacetate with propargyltrimethylsilane and Lewis acids led exclusively to the α-allene **4**.[20] The exchange of acetate protecting groups to benzyl ethers and ozonolysis afforded the α-aldehyde **7** that isomerized to the β-stereoisomer **8** under basic conditions.[19a] Both crude aldehydes **7** and **8** were converted to the corresponding phenyl ketones **9** and **10**[21] by addition of phenylmagnesium bromide followed by oxidation.[16b,22] Deprotection of the benzyl ethers and reduction of the ketone group of the intermediate **9** by catalytic hydrogenolysis[16b] gave the (α-D-galactosyl)phenylmethane **1**. Difluorination of α-phenyl ketone **9** was achieved by using neat Deoxo-Fluor

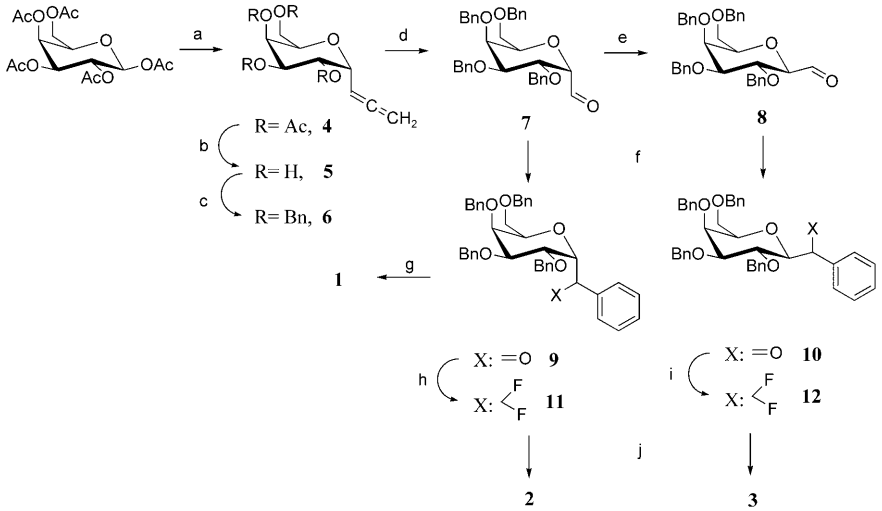

Scheme 1. Parallel Synthesis of compounds **1**, **2**, and **3**. a) propargyltrimethylsilane, $BF_3{\cdot}OEt_2$, TMSOTf, CH_3CN, 80%; b) NaOMe, MeOH, 90%; c) NaH, BnBr, nBu_4NI (cat.), DMF, 78%; d) O_3, CH_2Cl_2; e) Et_3N, *i*PrOH, CH_2Cl_2; f) i) PhMgBr, Et_2O, then aqueous work-up, ii) PCC, CH_2Cl_2 **9**: 50% for three steps, **10**: 25% for four steps; g) H_2, Pd/C 10% (cat.), MeOH, EtOAc, AcOH, 77%; h) neat Deoxo-Fluor, HF-pyridine (cat.), 80°C, 30 h, 77% (+8% SM); i) solution 50% Deoxo-Fluor in THF, HF-pyridine (cat.), 50–70°C, 20 h, 23% (+28% SM); j) H_2, Pd/C 10%, EtOH **2**: 70%, **3**: 67%. Deoxo-Fluor = bis(2-methoxyethyl)aminosulfur trifluoride, DMF = *N*,*N*-dimethylformamide, PCC = pyridinium chlorochromate, TMSOTf = trimethylsilyl trifluoromethanesulfonate.

reagent,[23] a catalytic amount of HF-pyridine, and heating to 80 °C for 30 h to afford the α-CF_2-protected sugar **11** in good yield. Under the same conditions of fluorination, the β-phenyl ketone **10** afforded the desired β-CF_2 analogue **12** in only 25 % yield along with 5 % unreacted starting material. No other product from the reaction mixture could be identified. In an attempt to improve the yield, β-phenyl ketone **10** was dissolved in a solution of 50 % Deoxo-Fluor in THF and was slowly heated from 50 °C to 70 °C to give the β-CF_2 analogue **12** in 23 % yield along with 28 % of starting material. Diluted Deoxo-Fluor in CH_2Cl_2 at 25 °C resulted in a very slow conversion of **10** to **12**. All further attempts to improve the yield of the above-mentioned reaction were unsuccessful. Finally, both **11** and **12** were benzyl deprotected by hydrogenolysis to give (α- and β-D-galactosyl)-(difluoro)phenylmethane **2** and **3**, respectively, which together with compound **1** were used for NMR spectroscopy studies in solution.

Table 1. Chemical shifts and coupling constants of compound **1** in CD_3OD (500 MHz, 298 K) and D_2O (500 MHz, 298 K).

H	$\delta(D_2O)$ [ppm]	$J(D_2O)$ [Hz]	$\delta(CD_3OD)$ [ppm]	$J(CD_3OD)$ [Hz]
H1	4.261	4.5 (H2), 3.5, 11.0	4.235	5.0 (H2), 4.5, 9.5
H2	4.040	4.5, 10.0	3.983	5.0, 8.8 (H3)
H3	3.896	3.5 (H4), 10.0 (H2)	3.844	8.8, 3.0 (H4)
H4	4.031	overlap	4.102	3.0, <0.5 (H5)
H5	4.021	overlap	4.021	5.2 (H6a), 7.0 (H6b)
H6a	3.643	5.0 (H5), −11.5	3.829	5.2, −11.3 (H6b)
H6b	3.597	7.5 (H5), −11.5	3.684	7.0, −11.3
CH_{2a}	2.991	11.0, −14.5	3.046	9.5 (H1), −14.5
CH_{2b}	2.978	3.5,−14.5	3.021	4.5 (H1), −14.5
H_{arom}	7.33	–	7.34	–

Table 2. Comparison between the experimental vicinal coupling constant values of **1** in CD_3OD (J_{exp}) and those calculated for the most stable conformations of the six-membered ring ($^4C_1$, $^1C_4$, $^1S_3$) according to MM3* calculations (J_{theor}).

Coupling constant		$^1C_4$	H-C-C-H torsion[b]	$^4C_1$	H-C-C-H torsion[b]	$^1S_3$	H-C-C-H torsion[b]
	ΔE[a] [kJ mol^{-1}]	9.81		0.00		3.17	
	J_{exp}[c] [Hz] CD_3OD	J_{theor}[b] [Hz]		J_{theor}[b] [Hz]		J_{theor}[b] [Hz]	
$J_{H1,H2}$	5.0	2.4	−55	3.9	43	2.1	−33
$J_{H2,H3}$	8.8	1.4	−67	8.7	172	7.2	−152
$J_{H3,H4}$	3.0	5.6	−53	5.0	54	3.9	62
$J_{H4,H5}$	<0.5	3.4	49	0.1	−57	2.4	−33
$J_{H5,H6b}$	7.0	9.5	−171	10.5	−176	9.5	−171
$J_{H5,H6a}$	5.2	4.2	−64	4.2	−65	4.2	−66
$J_{H1,CH2a}$	9.5	11.0	−177	11.4	174	10.9	−175
$J_{H1,CH2b}$	4.5	1.7	63	2.6	54	1.5	64

[a] The relative steric energy difference calculated by MM3* between the global minimum ($^4C_1$) and the other two major conformers is also given. [b] The theoretical values (J_{theor}) as well as the torsion angles were obtained by applying the generalized Karplus equation proposed by Altona to the geometries calculated by MM3* calculations. The gt conformer around the C5-C6 torsion was employed. [c] The comparison between the coupling constants indicates a predominant presence of the $^4C_1$ chair conformation. Moreover, there is a predominant conformation around the pseudoglycosidic linkage and around the C5-C6 torsion. In the latter case, there is also evidence for a non-negligible contribution of the alternative tg rotamer.

Conformational analysis

*Compound **1***: The analysis of the vicinal proton–proton coupling constants (Table 1 and Table 2) for the pyranose ring of **1** indicates a major presence of the $^4C_1$ chair conformation, as expected for natural galactosides.[24] The coupling values are very similar in CD_3OD and in D_2O solutions. Only this $^4C_1$ geometry can explain the observed couplings, whereas the calculated predictions for the alternative $^1C_4$ chair or the $^1S_3$ skew boat forms are far from the observed values. Furthermore, the presence of one large and one small–medium coupling constant between H1 and the two methylene protons indicates a major orientation around the glycosidic Φ torsion angle (defined as H1-C1-CH_2-C_{ipso}). The molecular mechanics MM3* calculations[25] also support these observations with the $^4C_1$ chair form being more than 3 kJ mol^{-1} more stable than the $^1S_3$ skew boat and much more stable than the alternative $^1C_4$ chair conformer. Regarding the orientation around the C5-C6 torsional bond, the intermediate observed $J_{H5,H6a}$ and $J_{H5,H6b}$ values (5.0–5.2 and 7.0–7.5 Hz) are in agreement with the typical gt:tg equilibrium observed for galactoside derivatives.[26]

The analysis of the NOE values[27] (Figure 1) supports the existence of the $^4C_1$ chair geometry as does that of an *exo*-anomeric-like orientation of the aromatic aglycon. The strong H1/CH_{2b}, H3/CH_{2a}, and H5/CH_{2a} NOE values for the methylene protons, together with the medium–strong H1/H_{arom} and H5/H_{arom} NOE values for the aromatic protons, can only be explained by a geometry in which the Φ torsion is −60° (Figure 2). Nevertheless, the comparison between the observed $J_{H1,\,CH2a}$ and $J_{H1,CH2b}$ with those calculated for a pure Φ −60° geometry is not perfect (Table 2), indicating the presence of rotamers (approximately 10–20 %) with the alternative Φ +60° geometry, which corresponds to a non-*exo*-anomeric orientation. These geometries have been also found in other *C*-glycosyl compounds.[28]

Molecular dynamics simulations of 5 ns (with the MM3* force field) were performed by using the global-minimum geometry as the input (Figure 2 and the Supporting Information). The results show that this conformer is fairly stable, with fluctuations along the well-defined Φ torsion value. Two sets of values (around +60° and −120°) are found for the Ψ angle (defined as C1-CH_2-C_{ipso}-C_{othro}). These values correspond to the symmetry that is inherent to a monosubstituted phenyl ring, for which the two *ortho* positions are chemically equivalent. The calculation of the ex-

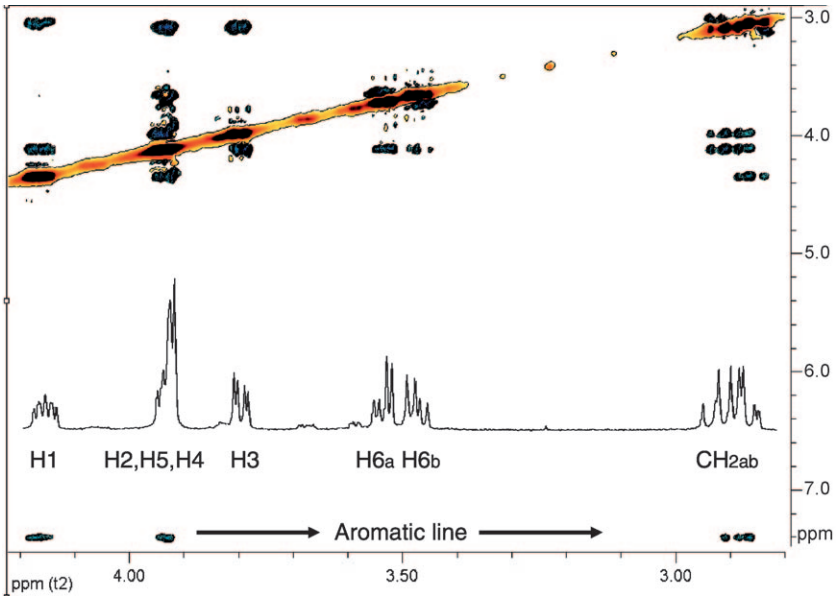

Figure 1. Section of the NOESY spectrum (500 MHz, 700 ms mixing time, D_2O, 298 K) showing the key NOE peaks and the 1D trace of the ^1H NMR spectrum. The cross-peaks indicate a major $^4C_1$ chair conformation as well as a major rotamer around Φ angle (H1-C1-CH_2-C_{ipso}). The cross-peaks are positive (different sign as diagonal peaks) as is expected for a small molecule. Indeed, the observed cross-peaks can be quantitatively fitted by using a correlation time of 50 ps.

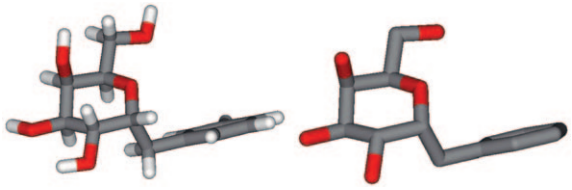

Figure 2. The major conformer of **1** (depicted with and without hydrogen atoms) according to the experimental NMR spectroscopic data and MM3* molecular mechanics and dynamics calculations. This orientation of the aromatic ring (defined by the Ψ angle) defines both orientations deduced by the MD simulations (+60° and −120°) owing to the intrinsic symmetry of the aromatic ring.

pected NOE values for the ensemble deduced by the MD simulations permitted us to quantitatively explain the observed NOE values (Table 3).[29]

According to the combined NMR spectroscopy and simulation data, **1** behaves as a mimetic of a natural galactose compound with a major $^4C_1$ chair conformation and an *exo*-anomeric orientation around Φ. To investigate its bioactivity, saturation transfer difference (STD) NMR spectra[30] of **1** together with the galactoside-specific VAA lectin were carried out in the molar ratio **1**:VAA of 50:1 (Figure 3). VAA lectin, which was isolated from the extracts of mistletoe, generally recognizes galactose moieties in α- and β-anomeric position and tolerates an aromatic aglycon well.[3a,18a,31] The STD experiments enabled us to deduce conclusions for the interactions between **1** and VAA lectin. Major saturation transfer to the protons in the pyranose ring was observed with basically no transfer to the methylene protons. Similar STD effects on the galactose peaks were observed.

Thus, the recognition mainly involved the galactose moiety. Moreover, competitive STD experiments by using lactose, a natural substrate for VAA, were performed. It was shown that **1** competed with lactose for the lectin site. The STD effects on **1** were clearly diminished when the haptenic inhibitor (lactose) was added to the NMR spectroscopy tube containing the synthetic compound and VAA. The binding affinity of **1** to VAA was estimated to be of the same order of magnitude to that of lactose, in the millimolar range, as the STD peak intensities on lactose were similarly affected upon addition of **1**.

Exchange transferred NOE experiments (trNOE) experiments were also applied to the

Table 3. Experimental NOE values for compound **1** in CD_3OD in comparison with those estimated by applying a full relaxation matrix approach to the major conformation.

Proton pair	NOEs %[a]	
	experimental (700 ms)	calculated (τ_c, 50 ps)
$H1/H_{arom}$	1.6	3.5
H1/H2	5.0	5.0
$H1/CH_{2b}$	2.9	3.2
$H5/CH_{2a}$	4.2	3.4
$H3/CH_{2a}$	4.3	3.7
H3/H4+H5	7.3	6.9
$H5/H_{arom}$	1.3	1.1
H6a/H4+H5	4.0	2.5
H6b/H4+H5	2.4	1.6

[a] The experiments (298 K) and the calculations (τ_c 50 ps, matched for the intra-residual H1/H2) were performed at 500 MHz. The agreement between experimental and theoretical values is satisfactory.

1:VAA sample, which had a molar ratio of 25:1. Strong negative signals were observed for this sample, even for short mixing times (100 and 200 ms), in contrast with the observation for the free state for which positive cross-peaks were observed in the NOESY spectrum. This clearly indicates the existence of binding and that the NOE peaks contain information on the bound state. The pattern of NOE peaks is basically identical to that measured for the free ligand (see Figure 1 and Figure 4), thus indicating that the lectin selects the $^4C_1$ major chair conformation of **1**. Selective experiments were carried out on specific signals of the ligand, namely the aromatic protons, H1, and the combined H2+H4+H5 signals (Figure 4). In particular, inversion of the anomeric proton H1 showed NOE signals at H2 and the methylene

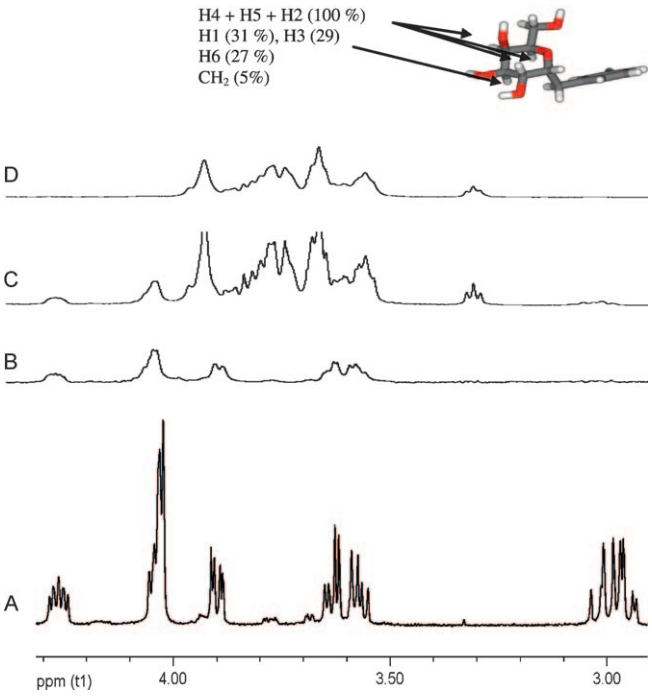

Figure 3. Compound **1** interacts with VAA lectin in an analogous manner to that of lactose, and with similar affinity, in the millimolar range. The concentration of the protein was approximately 25 μM. A) Section of the 500 MHz ^{1}H NMR spectrum of **1** B) STD spectrum of **1** (2 s saturation time) in the presence of VAA. The **1**:VAA molar ratio is 50:1. C) The STD spectrum of a 3:1 mixture of lactose:**1** added to the NMR tube containing VAA. The **1**:VAA molar ratio is again 50:1. D) The STD spectrum of a 100:1 mixture of lactose:VAA. The off-resonance frequency was set at 50 ppm while the on-resonance frequency was established at −0.5 ppm. The STD percentages are shown above in the corresponding caption of **1**.

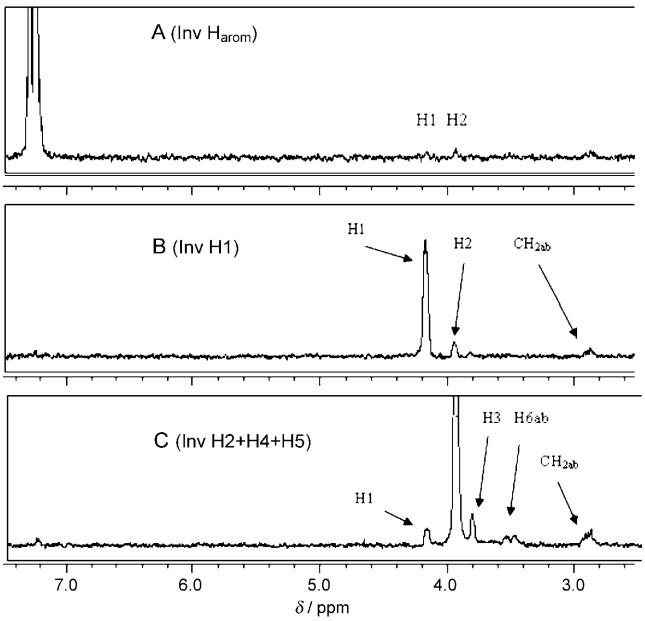

Figure 4. Selective 1D-trNOE experiments performed for a 25:1 mixture of **1**:VAA. The inverted signal in each case displays the highest intensity. A) Inversion of the aromatic protons. B) Inversion of the anomeric proton H1. C) Inversion of the resonance signal caused by H2, H4, and H5. The NOE signals have the same sign as the inverted signal, indicating binding of **1** to the lectin. The NOE pattern is basically identical to that observed in the free state (see NOESY in Figure 1), suggesting the presence of a bound $^4C_1$ conformation.

protons, but not at H6ab, suggesting that the $^1C_4$ chair is not bound. On the other hand, inversion of the aromatic protons showed negative NOE peaks at H1 and H2 protons, but these signals were very weak. This observation suggests that the aromatic protons still display flexibility in the bound state, probably owing to the lack of contact with the protein. This hypothesis was supported by docking calculations (see below).

To rationalize the interaction on the molecular level, the low-energy conformer, as observed by NMR spectroscopy, was docked into the VAA binding sites by the program AUTODOCK. Two sites are known in the lectin dimer, characterized by Trp38 in the 1α subdomain and by Tyr249 in the 2γ subdomain.[31] The $^4C_1$ conformer fitted very well in both cases (see Figure 9), much better than the alternative $^1C_4$ or skew boat conformers. In all cases, no contacts between the pseudoanomeric center and the lectin were predicted. Thus, docking analysis was in accordance with the NMR-derived observations.

*Compound **2***: The analysis of the vicinal proton–proton coupling constants (Table 4 and Table 5) for **2** indicates that no single conformation can fit the experimental data. The best fit is found when a combination of major $^1C_4$ and minor $^1S_3$ conformers are considered. Strikingly, the contribution of the regular $^4C_1$ present in natural galactosides is basically negligible.[32] This result is in complete contrast with the observations for the related GalaCH$_2$Ph analogue **1**. No conclusions about the conformation around the glycosidic linkage could be drawn owing to the lack of hydrogen atoms at the pseudoglycosidic CF$_2$ moiety. However, the presence of two similar $J_{H1,F}$ coupling constants (14.4 and 16.8 Hz) is in agreement with a high degree of conformational averaging around this Φ linkage (defined as H1-C1-CF$_2$-C$_{ipso}$). The conformation around Φ for a similar ManαCF$_2$R analogue was also recently described as a 77:23 *exo*/non-*exo* equilibrium, giving two coupling values of 14.3 and 19.4 Hz.[15] In

Table 4. Chemical shifts and coupling constants of compound **2** in CD$_3$OD (800 MHz, 298 K).[a]

H	δ [ppm]	J [Hz]
H1	4.401	3.2 (H2), 14.4 (F1), 16.8 (F2)
H2	3.880	3.2, 6.4 (H3)
H3	3.852	6.4, 3.2 (H4)
H4	4.161	3.2, 4.8 (H5)
H5	3.993	4.8, 4.0 (H6b), 7.2 (H6a)
H6a	3.834	7.2, −12.0
H6b	3.685	4.0, −12.0
H$_{ortho}$	7.583	–
H$_{meta+para}$	7.442	–

[a] The ^{1}H NMR spectrum of **2** in D$_2$O contains significant overlapping for the key peaks of the pyranose ring even at 800 MHz.

Table 5. Comparison between the experimental vicinal coupling constant values of **2** in CD_3OD (J_{exp}) and those expected for the most stable conformations of the six-membered ring ($^4C_1$, $^1C_4$, $^1S_3$) according to MM3*calculations (J_{theor}).

Coupling constant		$^1C_4$	H-C-C-H torsion[b]	$^4C_1$	H-C-C-H torsion[b]	$^1S_3$	H-C-C-H torsion[b]
	ΔE[a] [kJ mol^{-1}]	3.8		4.8		0.0	
	J_{exp}[c] [Hz] CD_3OD	J_{theor}[b] [Hz]		J_{theor}[b] [Hz]		J_{theor}[b] [Hz]	
$J_{H1,H2}$	3.2	*2.4*	−55.2	4.7	43.7	*3.2*	−33.8
$J_{H2,H3}$	5.6	*3.0*	−67.1	8.7	−172.5	*7.4*	−152.5
$J_{H3,H4}$	3.2	*3.4*	−54.0	5.0	54.8	*3.9*	62.9
$J_{H4,H5}$	4.8	*5.5*	49.1	0.1	−57.2	*2.4*	−33.0
$J_{H5,H6b}$	7.2	9.5	−171.6	10.0	176.6	9.5	−172.0
$J_{H5,H6a}$	4.0	1.9	70.3	2.5	65.1	2.0	69.6
$J_{H1,F1}$	14.4	–	−177	–	174	-	−175
$J_{H1,F2}$	16.8	–	63	–	54	–	64

[a] The relative steric energy difference calculated by MM3* between the global minimum ($^1S_3$) and the other two basic conformers is also given. [b] The theoretical values (J_{theor}), as well as the torsion angles, were obtained by applying the generalized Karplus equation proposed by Altona to the geometries calculated by MM3* calculations. The gt conformer around the C5–C6 torsion was employed. [c] The calculated couplings for the $^1C_4$ and the $^1S_3$ forms (italicized) are much closer to those observed experimentally than those expected for the $^4C_1$ geometry. The comparison between the couplings indicates that the contribution of the $^4C_1$ conformation is basically negligible. The best fit is given by an approximate 1:1 distribution between the $^1C_4$ and the $^1S_3$ conformers. Moreover, there is a predominant conformation around the pseudoglycosidic linkage and around the C5–C6 torsion. In the latter case, a non-negligible contribution of the alternative tg rotamer is tangible.

contrast, a 50:50 *exo*/non-*exo* equilibrium for an analogous molecule with a GalβCF_2R linkage produced two identical $J_{H1,F}$ coupling values of 14.3 Hz.[15] Although no Karplus-like relationship exists for this coupling pathway, the relatively similar $J_{H1,F1}$ and $J_{H1,F2}$ coupling constants observed for **2** indicate, beside the major *exo*-anomeric orientation, the presence of rotamers with the alternative Φ +60 non-*exo*-anomeric geometry. This molecule therefore displays a wide range of conformational flexibility, not only for the pyranose ring but also around the glycosidic Φ torsion.

Next, we probed into the issue on the origin and nature of the conformational flexibility. As the conformational entropy of six-membered $^1S_3$ skew-boat form is higher than those of the corresponding chair geometries, we addressed the issue as to whether there is an entropic origin for the detected flexibility. A series of ^1H NMR spectra was recorded at high field (800 MHz, to avoid interference from strong coupling effects) and at different temperatures and solvents to monitor the possible changes of coupling constants. In principle, the decreasing temperature should lead to a higher population of the enthalpically favored form, with a concomitant change in coupling-constant values. However, no change was observed for any of the intra-ring H/H couplings nor for the F-related $J_{H1,F}$ values (all differences were below 0.5 Hz). This indicates that the observed conformational flexibility does not necessarily correspond to intrinsic effects related to the conformational entropy of the molecule. Nevertheless, the change in temperature leads to a clear coalescence in the ^{19}F NMR spectra (see the Supporting Information), both in CD_3OD (at 273 K) and CD_3CN (at 243 K). The associated activation energy was approximately 15.0 kcal mol^{-1} in CD_3OD and 16.7 kcal mol^{-1} in CD_3CN, probably related to changes around the glycosidic torsions.

Furthermore, 5 ns MM3* molecular-dynamics simulations were performed by using the geometry of the three minima as input values (Figure 5 and the Supporting Information). The results indicated that the three conformers were fairly stable, with fluctuations along the well-defined Φ torsion value. Two sets of values (around +60° and −120°) were found for the Ψ angle (defined as C1-CF_2-C_{ipso}-C_{ortho}). These values corresponded to the symmetry inherent to a monosubstituted phenyl ring for which the two *ortho* positions are chemically equivalent. The

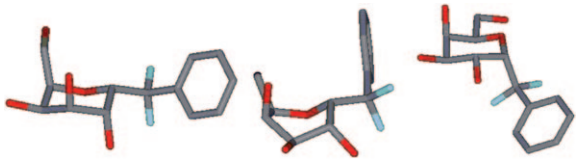

Figure 5. The major conformers of **2** (left, $^1C_4$; center, $^1S_3$) according to the experimental NMR data and MM3* molecular mechanics and dynamics calculations. The non-*exo*-anomeric form around Φ is depicted for the $^1C_4$ chair and the *exo*-anomeric geometry for the $^1S_3$ skew boat, respectively. The minor $^4C_1$ chair conformer (non-*exo*-anomeric orientation around Φ) is presented at the right side. This orientation of the aromatic ring (defined by Ψ angle) defines both orientations deduced by the MD simulations (+60° and −120°) owing to the intrinsic symmetry of the aromatic ring. NOE signals and J couplings are quantitatively accounted for by a 1:1 mixture of the $^1C_4$ and $^1S_3$ conformers.

calculation of predicted NOE values for a mixture of geometries computed from MD simulations starting from a mixture of the $^1C_4$ and $^1S_3$ conformers enabled us to quantitatively explain the observed NOE peaks (Table 6).

According to the combined NMR spectroscopy and simulation data, **2** does not appear to behave as a true mimetic of the natural compound. The natural major $^4C_1$ chair conformation is not present in solution and the *exo*-anomeric orientation around Φ coexists with the unusual non-*exo*-anomeric conformation.

Compound **2** was obtained as single crystals and its conformation determined in the solid state by X-ray crystallography (Figure 6). Strikingly, its conformation was that which is not present in methanol solution, that of the "natural" $^4C_1$ chair conformation. This is not a completely novel case. In several instances,[33] different conformations have been ob-

Table 6. Experimental NOE values for compound **2** in CD_3OD in comparison with those estimated by applying a full relaxation matrix approach to a 1:1 distribution of the $^1C_4$ and $^1S_3$ conformers.

Proton pair	NOEs %[a] experimental (700 ms)	calculated 1:1 $^1C_4$:$^1S_3$ distribution 50 ps correlation time)
$H1/H_{arom}$	1.3	3.5
H1/H2	4.4	4.4
H1/H6a	4.2	6.1
H5/H3	0.3	1.0
H3/H4	4.9	3.9
H4/H5	4.2	5.1
$H5/H_{arom}$	0.6	0.4
H6a/H5	1.1	0.7
H6b/H5	2.5	3.0

[a] The experiments (298 K) and the calculations (τ_c 50 ps, matched for the intraresidual H1/H2) were performed at 500 MHz. The agreement between calculation and experimental result is satisfactory.

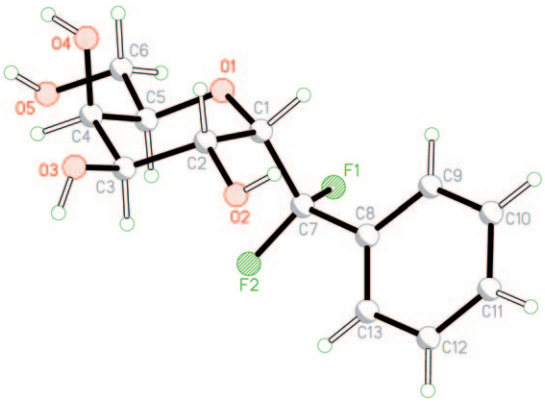

Figure 6. The $^4C_1$ chair geometry is obtained in the solid state after X-ray analysis of single crystals of **2**. The orientation of the aromatic ring corresponds to a non-*exo*-anomeric conformation.[34]

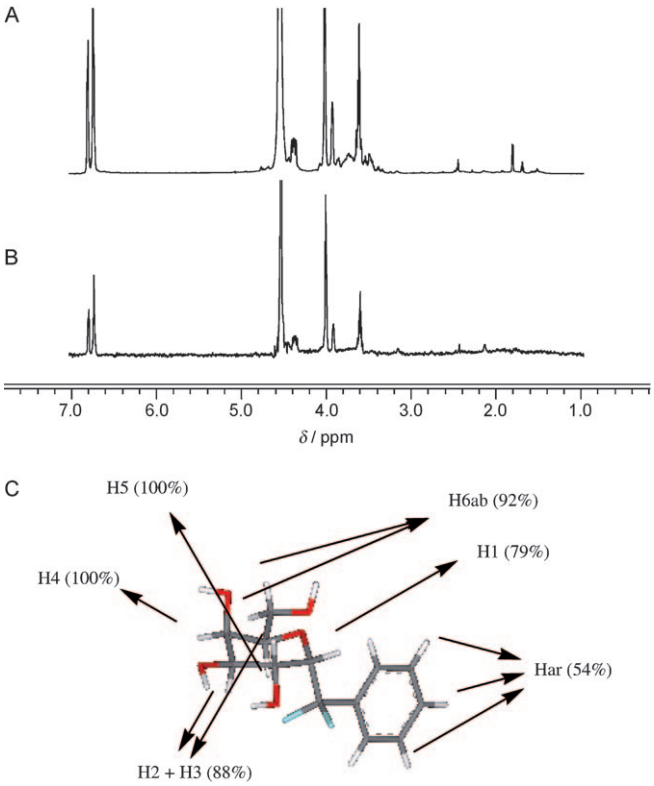

Figure 7. Compound **2** interacts with VAA lectin. A) This spectrum shows a section of the 500 MHz ^1H NMR spectrum of **2** in D_2O. B) STD spectrum of **2** (2 s saturation time) in the presence of VAA (approximately 25 μM). The **2**:VAA molar ratio is 50:1. The general STD spectrum also shows transfer to the aromatic protons. The off-resonance frequency was set at 50 ppm and the on-resonance frequency was established at −0.5 ppm. C) STD effects on the different proton atoms of **2**, as deduced from the STD experiments. 100% is given to the highest intensity (H4+H5), and all the other values are referred to this one. Analogous numbers are observed for all the compounds.

tained for sugar derivatives in solution than in the solid state. The key point is that this finding reveals intrinsic flexibility of glycomimetics of the *C*-glycosyl family, not only for the pseudoglycosidic linkages, but also at the level of the six-membered ring.

Having described structural properties, we next used STD NMR spectroscopic experiments to test the possible binding of **2** to VAA lectin. The lectin binds **2**, as observed in the STD experiment (Figure 7). Major saturation transfer is detected to the H2–H5 region, followed by the H1 and H6 areas. This indicates a clear interaction of this molecule with the lectin. Glycomimetic **2** also competed with lactose for the lectin site. The STD effects of **2** were clearly diminished when lactose was added to the VAA/**2** solution. In this case, the STD peaks of lactose were also affected upon addition of **2** to the corresponding VAA/lactose mixture, although to a lesser extent than that for the alternative experiment. Thus, it seems feasible to assume that the binding affinity of **2** is smaller (but still in the millimolar range) than that of the natural analogue, lactose. From the conformational perspective, it has been previously shown that lactose is selected by VAA in the *syn*-conformation.[32,33]

To define which conformation of compound **2** VAA lectin binds preferentially, a trNOE experiment (data not shown) was performed. As for the CORCEMA analysis[35] of the STD effects, the trNOE did not lead to conclusions on this issue. Owing to the signal overlapping of the key protons of **2** in D_2O, along with the small size of the ligand and the similarity of the observed STDs for the ring protons, only ambiguous conclusions could be drawn. Nevertheless, docking calculations (as for compound **1**) with the three standard conformations $^4C_1$, $^1C_4$, and $^1S_3$ of **2** suggested that the chair conformation $^4C_1$ fits VAA better than others, in which case compound **2** behaves like compound **1** when binding to VAA occurs.

Compound **3**: The chemical shifts and *J* coupling values of the β-linked CF_2 analogue **3** are compiled in Table 7. In this case, all the data are in close agreement with a major $^4C_1$ chair conformation in CD_3OD and D_2O solution. The two coupling values to the fluorine atom are in the medium

Table 7. Comparison between the experimentally observed coupling constants in CD_3OD for **3** (J_{exp}) and those expected for a $^4C_1$ chair conformation according to the MM3* force field (J_{theor}). Chemical shifts (δ, ppm) of **3** in CD_3OD (500 MHz, 298 K) are also given.

Coupling constant	J_{exp} CD_3OD [Hz]	$^4C_1$ J_{theor} [Hz]	H-C-C-H torsion	H	δ [ppm]
$J_{H1,H2}$	10.1	13.2	174.9	H1	3.70
$J_{H2,H3}$	8.4	8.7	−171.1	H2	3.73
$J_{H3,H4}$	3.6	2.5	54.5	H3	3.48
$J_{H4,H5}$	<1	0.6	−56.4	H4	3.87
$J_{H1,F1}$	9.4			H5	3.46
$J_{H1,F2}$	10.5			H6ab	3.62, 3.59

range, 9.4 and 10.5 Hz, indicating the possible presence of a conformational equilibrium around Φ torsion between the *exo* and non-*exo* orientations. Indeed, the steric energy difference (MM3* with GB/SA) between both forms amounts to only 1 kcal mol^{-1}. Strong NOE values are observed from the *ortho* aromatic protons to both H1 and H2, with a smaller NOE to H5. The simultaneous presence of these NOE values indicates the presence of an equilibrium between the *exo* and non-*exo* orientations, and the stronger NOE to H2 suggests that the second is the major conformer in solution. (see Figure 8 and the Supporting Information).

STD experiments performed under the same experimental conditions as for **1** and **2** indicated ligand binding to VAA lectin (data not shown), whereas the AUTODOCK calculations predicted the preferential binding of the major $^4C_1$ conformer (Figure 9). No preference for any of the three possible orientations around Φ, *exo*, non *exo*, and *anti*, was deduced.

Conclusion

The conformations of two α-linked and one β-linked *C*-glycosyl compounds were studied by using a combination of NMR spectroscopic and molecular-modeling procedures. These compounds, especially the α-linked analogues, harbor conformational flexibility. This appears around the pseudo-glycosidic linkages, but also in different geometries that are adopted by the six-membered ring, depending on the substitution at the pseudo-glycosidic carbon. It was found that CF_2 substitution at the α-anomeric position resulted in significant flexibility of the six-membered ring in solution. The conformation of the ring observed in the solid state of this molecule had an almost negligible population in solution. The inherent flexibility of ligands can have implications from the molecular recognition viewpoint and, when interacting with protein receptors, conformational selection processes usually take place, given the relatively low-energy barriers required for conformer interconversion.[33] However, despite the different conformational behavior, certain *C*-galactosyl analogues might still be recognized by galactose-binding proteins, as exemplified here by using VAA. The detection of

Figure 8. Compound **3** shows a major $^4C_1$ conformation in solution, in contrast with the behavior of its α-linked analogue, compound **2**. The observed NOE peaks suggest that the orientation of the aromatic ring is that shown at the lefthand side of the Figure (non-*exo*-anomeric), although the alternative one (*exo*-anomeric, right) seems to be also present in solution.

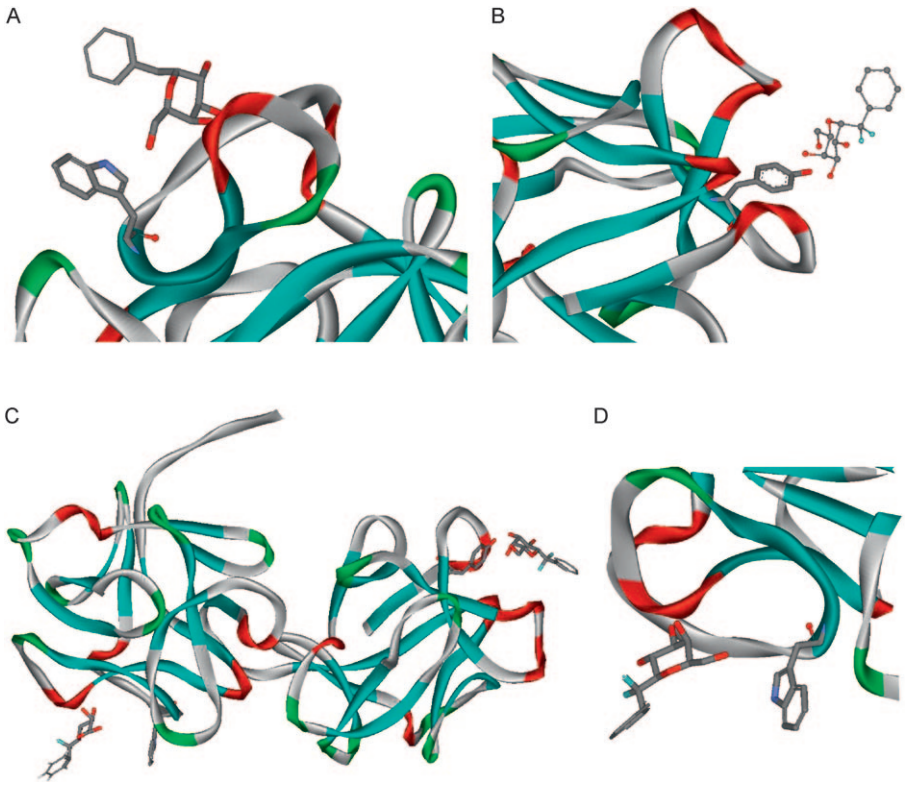

Figure 9. Different views of the putative binding mode of compounds **1**–**3** to VAA, according to AUTODOCK calculations. A) Expansion of the Trp site of VAA, showing the interaction with **1** in the preferred $^4C_1$ chair conformation. B) Expansion of the Tyr-site of VAA, showing the interaction with **2** in the $^4C_1$ chair conformation. C) Compound **3** bound to the complete VAA lectin, showing both sites. D) Expansion of the Trp site of VAA, showing the interaction with **3** in the preferred $^4C_1$ chair conformation.

binding will give further research a clear direction in the design of potent non-hydrolyzable mimics for medically relevant lectins.

Experimental Section

Modeling: The low energy conformers were calculated by using the MM3* force field[25] in the program MAESTRO.[36]

The torsion angle Φ is defined as $H1_{Gal}$-$C1_{Gal}$-C-C_{ipso} and Ψ as $C1_{Gal}$-C-C_{ipso}-C_{ortho}. The three possible staggered rotamers around Φ combined with those for Ψ (every 120°) were built (nine conformers in total) with MAESTRO and submitted to exhaustive energy minimization. The probability distribution was calculated from the obtained energy values according to a Boltzmann function at 300 K. In all the molecular mechanics and dynamics calculations, the GB/SA solvation model for water was used.[37]

For the α-CF_2 analogue **2**, for which the $^3J_{H,H}$ coupling analysis showed the presence of distinct six-membered ring geometries present in solution, three different starting geometries were considered, corresponding to the $^4C_1$ chair, $^1C_4$ chair, and $^1S_3$ skew boat. Thus, in total, 27 conformers were calculated. For the α-CH_2 analogue **1** and the β-CF_2 analogue **3**, only the $^4C_1$ chair conformation was considered as the $^3J_{H,H}$ coupling values were in agreement with the exclusive presence of this conformer.

The molecular dynamics simulations were also performed by using the MM3* force field. For molecular dynamics simulations, the global-minimum geometry was used as input. A temperature of simulation of 300 K was employed with a time step of 1.5 fs and an equilibration time of 100 ps. The total simulation times for each compound were 5 ns.

For the C5-C6 torsion, only the gt geometry (ω, defined as C4-C5-C6-O4 ca. 180°) was considered as it has been demonstrated to be the major conformation for galactose derivatives (O4 in axial orientation).[26]

NMR experiments: ^{1}H NMR (800 MHz) spectra of compound **2** were recorded on a Bruker AVANCE 800 spectrometer (CryoProbe). Three different solvents were used: CD_3OD, CD_3CN, and D_2O. For every solvent, a series of spectra at variable temperatures ranging from 0°C to +50°C (for D_2O: +10°C to +50°C) were measured at concentrations of 30 mM. Chemical shifts are reported in ppm, after calibration of the residue peak of each solvent: $\delta = 3.31$ ppm for CD_3OD, $\delta = 1.94$ ppm for CD_3CN, and $\delta = 4.79$ ppm for D_2O. Vicinal proton–proton coupling constants were estimated from first-order analysis of the spectra recorded at 800 MHz to minimize strong-coupling effects.

^{1}H NMR (500 MHz) spectra were recorded at 30°C in D_2O and in CD_3OD on a Bruker AVANCE 500 spectrometer. Concentrations of approximately 2 mM of **1**, **2**, and **3** were used. Chemical shifts are reported in ppm by using external TSP (2,2,3,3-tetradeutero-3-trimethylsilylpropionic acid, 0 ppm) as the reference. The 2D-TOCSY experiment (30 ms mixing time) was performed by using a data matrix of 256×2 K to digitize a spectral width of 4000 Hz. Four scans were used per increment with a relaxation delay of 2 s. 2D-NOESY (600 and 1000 ms) and 2D-T-ROESY experiments (400 and 500 ms) used the standard sequences. Distances were estimated from NOESY/ROESY experimental data by using the average values of the isolated spin-pair approximation[38] for the data with the shorter mixing time. Estimated errors are below 10%.

A comparison between the observed NOE values and those estimated for the different conformations was performed by using a full relaxation matrix approach and a home-made program, which is available from the authors upon request.[39] For all molecules, an average effective correlation time of 50 ps was estimated for the best adjustment of the observed and calculated cross-peaks.

Interaction studies with VAA lectin: The lectin was isolated from the extracts of dried mistletoe leaves by using affinity chromatography on lactosylated Sepharose 4B as crucial step. Purity and quaternary structure were ascertained by one- and two-dimensional gel electrophoresis, gel filtration and ultracentrifugation and carbohydrate-dependent activity was tested by haemagglutination as well as solid-phase/cell assays.[3c,39,40]

The binding of the galactose analogues was evaluated by STD experiments. STD experiments were performed without saturation of the residual HDO signal for molar ratios 50:1 of compound:VAA. The concentration of the protein was approximately 25 μM. A series of Gaussian-shaped pulses of 50 ms each was employed with a total saturation time for the protein envelope of 2 s and a maximum $B1$ field strength of 60 Hz. An off-resonance frequency of $\delta = 40$ ppm and on-resonance frequency of $\delta = -1.0$ ppm (protein aliphatic signals region) were applied. In the case of the CH_2-analogue **1**, competition experiments with lactose were also performed. In this case, a threefold excess of lactose was added to the NMR tube of the sample containing VAA/**1**, and the STD experiment was performed by using the same experimental conditions described above. For compounds **2** and **3**, analogous experiments were performed.

For the VAA/**1** sample, exchange trNOE experiments[41] were performed by using selective 1D experiments with the double-pulse field-gradient spin-echo (DPFGSE) module.[42] Measurements were done with a freshly prepared ligand/lectin mixture, with mixing times of 100 and 200 ms, at an approximately 20:1 molar ratio of ligand/protein. A concentration of 2 mM of the ligand was employed in all cases. No purging spin-lock period was employed to remove the NMR signals of the macromolecule background. Strong negative NOE cross-peaks were observed, which is in contrast with the free state and indicates binding of the sugars to the lectin preparation. trNOE experiments were also attempted for the VAA/**2** and VAA/**3** samples, but they did not afford additional information owing to the extensive overlapping of the key signals.

Docking calculations: The $^4C_1$ and $^1C_4$ chair conformers of **1**–**3** (as observed by NMR spectroscopy) were manually docked into the two carbohydrate-binding sites of VAA in the 1α and 2γ subdomains of the B subunit of VAA[43] by superimposing the terminal Gal residue (protein database code 1PUM). Then, different possibilities of arranging the side chain of the glycan were used as input geometries for AutoDock 3.0 simulations[44] with the multiple Lamarckian Genetic Algorithm. Only local searches were performed centered in the two experimental galactoside-specific VAA X-ray sites. Grids of probe atom interaction energies and electrostatic potential were generated by the AutoGrid program present in AutoDock 3.0. Grid spacings of 0.6 and 0.375 Å were used for the global and local searches, respectively. For each calculation, 100 docking runs were performed by using a population of 200 individuals and an energy evaluation number of $3x10^6$. The best scoring was always obtained with the $^4C_1$ chair conformer, independently of the anomeric configuration of **1**–**3**.

Synthesis

General: Commercial reagents (Fluka, Aldrich, Acros) were used without purification. CH_2Cl_2 and THF were dried from activated alumina columns (IT technology). The other anhydrous solvents were purchased and stored over molecular sieves. CAUTION! Neat Deoxo-Fluor reagent is thermally unstable[23a] over 150°C and it reacts violently with water, therefore it should be handled carefully, under a well ventilated hood, and behind a safety shield. Flash column chromatography (FC): Fluka silica gel, No.60752, 230–400 mesh. TLC for reaction monitoring: Merck silica gel 60 F_{254} plates; detection by UV light; Pancaldi reagent or $KMnO_4$ solution. Melting Points (m.p.): Büchi SMP-20; uncorrected. Optical rotations ($[\alpha]_D^{25}$): Jasco P-1020; lamp Na, 589 nm; 25°C. IR spectra: Perkin Elmer Paragon 1000 or Perkin Elmer Spectrum One FT-IR Spectrometer. NMR spectra: Bruker ARX-400 or DPX-400 Spectrometer, 400 MHz for ^{1}H, 100.6 MHz for ^{13}C and 376.7 MHz for ^{19}F; δ for ^{1}H NMR and ^{13}C NMR in ppm relative to the solvent's residual signal as the internal reference [$CDCl_3$, δ(H) 7.26 and δ(C) 77.0, CD_3OD, δ(H) 3.31 and δ(C) 49.0, D_2O δ(H) 4.79], δ for ^{19}F NMR in ppm relative to signal of external reference [$CFCl_3$, δ(F) 0]; all ^{1}H and ^{13}C assignments were confirmed by 2D-COSY and 2D-HSQC spectra. Mass spectra (MS): Shimadzu Axima CFRplus for MALDI-TOF or Waters CapLC-coupled Micromass Ultima for ESI QqTOF. Elemental analyses: Ilse Beetz, D-96301 Kronach, Germany.

The atom numbering in NMR spectra follows the standard numbering for sugars, whereas the numbers in the compound name are generated according to IUPAC rules.

CCDC-683094 (**2**) contains the supplementary crystallographic data for this paper. These data can be obtained free of charge from The Cambridge Crystallographic Data Centre via www.ccdc.cam.ac.uk/data_request/cif.

2,6-Anhydro-1,3,4,5-tetra-*O*-acetyl-7,8,9-trideoxy-D-*glycero*-L-*galacto*-non-7,8-dienitol (4): $BF_3{\cdot}Et_2O$ (35.0 mL, 39.6 g, 0.279 mol) was added dropwise to a stirred solution of β-D-galactose pentaacetate (36.2 g, 0.093 mol) and propargyltrimethylsilane (28.0 mL, 21.0 g, 0.187 mol) in anhydrous CH_3CN (200 mL) at 0 °C under argon. This was then followed by the dropwise addition of TMSOTf (33.6 mL, 41.3 g, 0.186 mol). The reaction mixture was stirred at the same temperature for 2.5 h. Then, it was diluted with EtOAc (200 mL) and aqueous HCl 1 M (200 mL) was added. The two phases were separated and the aqueous phase was extracted with EtOAc (150 mL × 2). The combined organic phases were washed with saturated aqueous $NaHCO_3$ and brine until a neutral pH value was obtained, dried over Mg_2SO_4, and concentrated in vacuo. FC (25% EtOAc in petroleum ether) afforded **4** as a yellowish solid (27.5 g, 80%). Part of this solid was recrystallized from Et_2O and *n*-hexane to afford colorless crystals of **4**. m.p. 77–79 °C; $[\alpha]_D^{25} = +186$ ($c = 0.185$, MeOH); IR (neat): $\tilde{\nu} = 1956$ (allene), 1736, 1724 (C=O of AcO), 1227, 1210, 1091, 1049, 1018, 910, 878 cm^{-1}; ^1H NMR (400 MHz, $CDCl_3$, 298 K): $\delta = 5.43$ (dd, 1H, $^3J_{H4,H3} = 3.3$ Hz, $^3J_{H4,H5} = 1.5$ Hz, H4), 5.35 (dd, 1H, $^3J_{H2,H3} = 10.5$ Hz, $^3J_{H2,H1} = 5.5$ Hz, H2), 5.23–5.28 (m, 1H, HC=), 5.25 (dd, 1H, $^3J_{H3,H2} = 10.7$ Hz, $^3J_{H3,H4} = 3.3$ Hz, H3), 4.91–4.95 (m, 3H, $=CH_2$, H1), 4.24 (ddd, 1H, $^3J_{H5,H6a} = 6.8$ Hz, $^3J_{H5,H6b} = 6.2$ Hz, $^3J_{H5,H4} = 1.2$ Hz, H5), 4.12 (dd, 1H, $^2J_{H6b,H6a} = 11.1$ Hz, $^3J_{H6b,H5} = 6.2$ Hz, H6b), 4.07 (dd, 1H, $^2J_{H6a,H6b} = 11.1$ Hz, $^3J_{H6a,H5} = 7.4$ Hz, H6a), 2.15, 2.06, 2.04, 2.00 ppm (4 s, 12H, 4× CH_3 of AcO); ^{13}C NMR (100 MHz, $CDCl_3$, 298 K): $\delta = 209.2$ (=C=), 170.3, 170.1, 170.0, 169.7 (4×C=O of AcO), 84.4 (HC=), 77.5 ($=CH_2$), 70.7 (C1), 68.2 (C5), 68.0 (C3, C4), 67,6 (C2), 61.8 (C6), 20.6 ppm (CH_3 of AcO); ESI QqTOF-MS: calcd for ([*M*+Na]) 393.1162, found 393.1167.

2,6-Anhydro-7,8,9-trideoxy-D-*glycero*-L-*galacto*-non-7,8-dienitol (5): A solution of 30% MeONa in MeOH (1.80 mL, 0.52 g, 0.0097 mol) was added dropwise at 25 °C to a stirred solution of allene **4** (30.0 g, 0.081 mol) in MeOH (450 mL). After the mixture had been stirred at the same temperature for 2 h, Dowex 50WX8 (50–100 mesh) was added in small portions until the pH value of the reaction mixture became neutral. After 15 min, it was filtered and concentrated in vacuo. The residue was recrystallized from MeOH to afford **5** as white crystals (14.7 g after three recrystallizations, 90%). M.p. 153–157 °C; $[\alpha]_D^{25} = +243$ (c = 0.175, MeOH); IR (neat): $\tilde{\nu} = 3675$, 3429, 3227 (br, HO), 1948 (allene), 1077, 1060, 1026, 999, 786 cm^{-1}; ^1H NMR (400 MHz, D_2O, 298 K): $\delta = 5.47$ (ddd, 1H, $^4J_{HC=,=CH2a} = {}^4J_{HC=,=CH2b} = {}^3J_{HC=,H1} = 6.7$ Hz, HC=), 4.96 (ddd, 1H, $^2J = 11.8$ Hz, $^4J_{=CH2a,HC=} = 6.8$ Hz, $^5J_{=CH2a,H1} = 2.7$ Hz, $=CH_{2a}$), 4.92 (ddd, 1H, $^2J = 11.7$ Hz, $^4J_{=CH2b,HC=} = 6.6$ Hz, $^5J_{=CH2b,H1} = 2.7$ Hz, $=CH_{2b}$), 4.65–4.69 (m, 1H, H1), 4.04 (dd, 1H, $^3J_{H2,H3} = 10.3$ Hz, $^3J_{H2,H1} = 6.2$ Hz, H2), 3.96–4.01 (m, 2H, H5, H4), 3.81 (dd, 1H, $^3J_{H3,H2} = 10.3$ Hz, $^3J_{H3,H4} = 3.2$ Hz, H3), 3.70 ppm (d, 2H, $^3J_{H6,H5} = 6.0$ Hz, H6a,b); ^{13}C NMR (100 MHz, CD_3OD in D_2O, 298 K): $\delta = 210.8$ (=C=), 85.1 (HC=), 77.5 ($=CH_2$), 75.3 (C1), 73.7 (C5 or C4), 71.0 (C3), 70.4 (C5 or C4), 69.0 (C2), 62.2 ppm (C6); ESI QqTOF-MS: calcd for ([*M*+Na]) 225.0739, found 225.0741.

2,6-Anhydro-1,3,4,5-tetra-*O*-benzyl-7,8,9-trideoxy-D-*glycero*-L-*galacto*-non-7,8-dienitol (6): The solid allene **5** (1.00 g, 4.94 mmol) was added in small portions to a vigorously stirred suspension of NaH (60% of purity, 0.90 g, 22.5 mmol, previously washed with anhydrous pentane under argon) in anhydrous *N*,*N*-dimethylformamide (DMF; 20 mL) at 0 °C under a flow of argon. After completion of the addition, the thick suspension was stirred for 45 min at 25 °C. Catalytic amount of nBu_4NI (0.20 g, 0.54 mmol) was added, followed by the dropwise addition of BnBr (3.2 mL, 4.6 g, 27 mmol) at 0 °C. After the completion of the addition, the reaction mixture was stirred at 25 °C for an additional 16 h. Then, the reaction was quenched by careful addition of MeOH (3 mL) at 0 °C. The mixture was partitioned between Et_2O (50 mL) and water (50 mL), the two phases were separated and the aqueous phase was extracted with Et_2O (3×30 mL). The combined organic phases were dried over $MgSO_4$ and concentrated in vacuo. Most of the DMF was removed under high vacuum and the residue was purified by FC (10% Et_2O in petroleum ether) to afford **6** (2.17 g, 78%) as a colorless oil that has identical spectroscopic data to those previously reported.[19a] $[\alpha]_D^{25} = +95$ ($c = 0.18$, $CHCl_3$).

2,6-Anhydro-3,4,5,7-tetra-*O*-benzyl-D-*glycero*-L-*gluco*-heptose (7) and 2,6-anhydro-3,4,5,7-tetra-*O*-benzyl-D-*glycero*-L-*manno*-heptose (8): Compounds **7** and **8** were prepared as previously reported[19a] and used in the next steps as crude mixtures.

2,6-Anhydro-3,4,5,7-tetra-*O*-benzyl-1-*C*-phenyl-a*ldehydo*-D-*glycero*-L-*gluco*-heptose (9): PhMgBr solution in Et_2O (ca. 3 M, 1.5 mL, 4.5 mmol) at −78 °C under argon was added dropwise to a stirred solution of the crude α-aldehyde **7** (1.73 mmol) in anhydrous THF (22 mL). The reaction mixture was kept at the same temperature for 1.5 h. It was warmed up to −20 °C over an additional 2 h. Then, the reaction was quenched by pouring the mixture into a pH 7 phosphate buffer solution 0.05 M (30 mL) and the mixture was filtered through Celite. The filtrate was extracted with Et_2O (4×25 mL) and the combined organic phases were dried over $MgSO_4$ and concentrated in vacuo to afford a mixture of alcohols that were then used without purification. Activated 4 Å molecular sieves (≈1.6 g) and pyridinium chlorochromate (PCC; 1.87 g, 8.67 mmol) were added in one portion to a vigorously stirred solution of the previous crude mixture in anhydrous CH_2Cl_2 (24 mL) at 25 °C and under argon. The reaction mixture was stirred at the same temperature for 2 h. Then Et_2O (100 mL) was added and the mixture was left without stirring. After 30 min, the upper solution was filtered through a pad of florisil. The black tar that precipitated was washed several times with Et_2O and filtered as well. The filtrate was concentrated in vacuo and purified by FC (15% Et_2O in petroleum ether) to afford ketone **9** as a yellowish oil (0.54 g, 50% for three steps starting from the α-allene **6**). $[\alpha]_D^{25} = +35$ ($c = 0.184$, $CHCl_3$); IR (neat): $\tilde{\nu} = 1694$, 1682 (C=O), 1597, 1496, 1455, 1372, 1217, 1094, 732 cm^{-1}; ^1H NMR (400 MHz, $CDCl_3$, 298 K): $\delta = 7.90$–7.93 (m, 2H), 7.50–7.55 (m, 1H), 7.24–7.40 (m, 17H), 7.16–7.22 (m, 3H), 7.03–7.07 (m, 2H) H_{arom}, 5.20 (d, 1H, $^3J_{H1,H2} = 4.3$ Hz, H1), 4.74 (d, 1H, $^2J = 11.7$ Hz), 4.73 (d, 1H, $^2J = 12.0$ Hz), 4.66 (d, 1H, $^2J = 12.0$ Hz), 4.57 (d, 1H, $^2J = 11.7$ Hz), 4.55 (d, 1H, $^2J = 12.0$ Hz), 4.47 (d, 1H, $^2J = 12.0$ Hz), 4.47 (br s, 2H) 4×CH_2 of BnO, 4.37 (ddd, 1H, $^3J_{H5,H6a} = 8.0$ Hz, $^3J_{H5,H6b} = 4.5$ Hz, $^3J_{H5,H4} = 3.5$ Hz, H5), 4.20 (dd, 1H, $^3J_{H2,H3} = 6.8$ Hz, $^3J_{H2,H1} = 4.1$ Hz, H2), 4.14 (dd, 1H, $^3J_{H3,H2} = 6.8$ Hz, $^3J_{H3,H4} = 2.5$ Hz, H3), 4.10 (dd, 1H, $^3J_{H4,H5} = 3.6$ Hz, $^3J_{H4,H3} = 2.8$ Hz, H4), 3.88 (dd, 1H, $^2J_{H6a,H6b} = 10.6$ Hz, $^3J_{H6a,H-5} = 7.6$ Hz, H6a), 3.66 ppm (dd, 1H, $^2J_{H6b,H6a} = 10.6$ Hz, $^3J_{H6b,H5} = 4.8$ Hz, H6b); ^{13}C NMR (100 MHz, $CDCl_3$, 298 K): $\delta = 197.6$ (C=O), 138.5, 138.4, 138.2, 137.9, 136.5 (C_{ipso} of Ph and BnO), 133.0, 129.0, 128.4, 128.3, 128.2, 127.95, 127.9, 127.7, 127.67, 127.6, 127.54, 127.5 (C_{arom}), 77.0 (C3), 76.2 (C2), 74.2 (C5), 73.9 (C4, CH_2 of BnO), 73.2, 73.1, 73.0 (3×CH_2 of BnO), 72.3 (C1), 66.9 ppm (C6); MALDI-TOF MS: calcd for ([*M*+K]) 667.2462, found 667.2457; elemental analysis calcd (%) for $C_{41}H_{40}O_6$ C 78.32, H 6.41; found: C 78.36, H 6.47.

2,6-Anhydro-3,4,5,7-tetra-*O*-benzyl-1-*C*-phenyl-*aldehydo*-D-*glycero*-L-*manno*-heptose (10): Compound **10** was prepared in the same way as described for its α-epimer **9**, starting from the crude β-galactosyl carbaldehyde **8** (0.94 mmol). FC (7.5% EtOAc in petroleum ether) gave **10** as a white solid (0.15 g, 25% for four steps starting from the α-allene **6**), which was recrystallized from cyclohexane. M.p. 104–105 °C [ref. [21] 103–105 °C]; $[\alpha]_D^{25} = +6.2$ ($c = 0.13$, $CHCl_3$) [ref. [21] +7.5 ($c = 0.8$, $CHCl_3$)]. The spectroscopic data are identical to those previously reported.[21]

2,6-Anhydro-7-deoxy-7-*C*-phenyl-D-*glycero*-L-*galacto*-heptitol (1): To a solution of ketone **9** (0.141 g, 0.22 mmol) in a mixture of MeOH (4 mL) and EtOAc (4 mL) was added Pd/C 10% (0.060 g) under argon, along with three drops of AcOH. Argon was exchanged for H_2 gas and the reaction mixture was stirred under an H_2 atmosphere (1 atm) at 25 °C for two days. Then, the mixture was filtered carefully through Celite and the filtrate was concentrated in vacuo. The residue was purified by FC (10% MeOH in CH_2Cl_2) to give **1** (0.044 g, 77%) as a colorless oil. $[\alpha]_D = +78$ ($c = 0.175$, MeOH); IR (neat): $\tilde{\nu} = 3306$, 2922 (br, OH), 1452, 1361, 1071, 1031, 978, 865, 778, 740, 697 cm^{-1}; ^1H NMR (400 MHz, CD_3OD, 298 K): $\delta = 7.23$–7.28 (m, 4H, H_{ortho}, H_{meta}), 7.14–7.18 (m, 1H, H_{para}), 4.14 (ddd, 1H, $^3J_{H1,CH2a} = 8.6$ Hz, $^3J_{H1,H2} \approx {}^3J_{H1,CH2b} \approx 5.4$ Hz, H1), 4.02 (br dd, 1H, $^3J_{H4,H3} \approx 3.2$ Hz, $^3J_{H4,H5} \approx 2.7$ Hz, H4), 3.94 (ddd, 1H, $^3J_{H5,H6a} = 6.5$ Hz, $^3J_{H5,H6b} = 5.4$ Hz, $^3J_{H5,H4} = 2.7$ Hz, H5), 3.90 (dd, 1H, $^3J_{H2,H3} = 8.6$ Hz,

$^3J_{H2,H1}=4.9$ Hz, H2), 3.74 (dd, 1H, $^3J_{H3,H2}=8.6$ Hz, $^3J_{H3,H4}=3.2$ Hz, H3), 3.67–3.74 (m, 1H, H6a), 3.67 (dd, 1H, $^2J_{H6b,H6a}=11.3$ Hz, $^3J_{H6b,H5}=5.4$ Hz, H6b), 2.91–2.97 ppm (m, 2H, CH_2); ^{13}C NMR (100 MHz, CD_3OD, 298 K): $\delta=140.9$ (C_{ipso}), 130.4, 129.2 (C_{ortho}, C_{meta}), 127.0 (C_{para}), 77.5 (C1), 74.4 (C5), 72.0 (C3), 70.1 (C2), 69.9 (C4), 61.7 (C6), 32.2 ppm (CH_2); ESI QqTOF MS: calcd for ([*M*+H]) 255.1232, found 255.1231; elemental analysis calcd (%) for $C_{13}H_{18}O_5$: C 61.40, H 7.14; found: C 61.30, H 7.14.

2,6-Anhydro-1-deoxy-1,1-difluoro-3,4,5,7-tetra-*O*-benzyl-1-*C*-phenyl-D-*glycero*-L-*gluco*-heptitol (11): In a PET vial containing the α-ketone **9** (0.50 g, 0.80 mmol), was added neat Deoxo-Fluor reagent (1.50 mL, 1.8 g, 8.1 mmol), followed by two drops of HF-pyridine as catalyst at 25°C under argon. The reaction was heated to 80°C for 10 h. More reagent was then added (0.30 mL, 0.36 g, 1.6 mmol) and the mixture was heated to 80°C for an additional 10 h. Further reagent was then added (0.15 mL, 0.18 g, 0.8 mmol) and heated to the same temperature for an additional 10 h. Then, the reaction mixture was added dropwise to a mixture of saturated aqueous $NaHCO_3$ and ice. It was allowed to reach 25°C and was extracted with Et_2O (3×30 mL). The combined organic phases were washed with brine, dried over $MgSO_4$, and concentrated in vacuo. The residue was purified by FC (15% Et_2O in petroleum ether) to afford **11** (0.40 g, 77%, 8% of starting material was also recovered) as a pale yellow oil. $[\alpha]_D=+59$ ($c=0.165$, $CHCl_3$); IR (neat): $\tilde{\nu}=1496$, 1454, 1372, 1270, 1205, 1094, 1028, 914, 735 cm^{-1}; ^1H NMR (400 MHz, $CDCl_3$, 298 K): $\delta=7.53$–7.56 (m, 2H), 7.23–7.37 (m, 17H), 7.15–7.21 (m, 4H), 7.11–7.14 (m, 2H) H_{arom}, 4.59 (d, 1H, $^2J=12.0$ Hz), 4.53 (d, 1H, $^2J=12.9$ Hz), 4.51 (brs, 2H), 4.45 (d, 1H, $^2J=12.0$ Hz) CH_2 of BnO, 4.39–4.42 (m, 1H, H5), 4.40 (d, 1H, $^2J=12.0$ Hz), 4.27 (d, 1H, $^2J=12.0$ Hz) CH_2 of BnO, 4.23–4.29 (m, 1H, H1), 4.16 (d, 1H, $^2J=12.0$ Hz, CH_2 of BnO), 4.11 (dd, 1H, $^3J_{H4,H5}=5.5$ Hz, $^3J_{H4,H3}=2.8$ Hz, H4), 3.88 (dd, 1H, $^3J_{H2,H3}\approx4.6$ Hz, $^3J_{H2,H1}\approx1.9$ Hz, H2), 3.83 (dd, 1H, $^2J_{H6a,H6b}=11.8$ Hz, $^3J_{H6a,H5}=8.2$ Hz, H6a), 3.74 (dd, 1H, $^3J_{H3,H2}=4.9$ Hz, $^3J_{H3,H4}=2.8$ Hz, H3), 3.71 ppm (dd, 1H, $^2J_{H6b,H6a}=12.0$ Hz, $^3J_{H6b,H5}=2.8$ Hz, H6b); ^{13}C NMR (100 MHz, $CDCl_3$, 298 K): $\delta=138.5$, 138.2, 138.1, 137.8 C_{ipso} of BnO, 136.1 (t, $^2J_{C,Fa}=^2J_{C,Fb}=25.7$ Hz, C_{ipso} of Ph), 129.8, 128.35, 128.3, 128.2, 128.1, 127.8, 127.7, 127.6, 127.5, 127.3 C_{arom} of BnO, 125.7 (t, $^3J_{C,Fa}=^3J_{C,Fb}=6.4$ Hz, C_{ortho} of Ph), 120.8 (dd, $^1J_{C,Fa}=253$ Hz, $^1J_{C,Fb}=245$ Hz, CF_2), 75.6 (C5), 75.0 (C3), 74.4 (C2), 73.3 (CH_2 of BnO), 73.2 73.15 (C4, CH_2 of BnO), 72.9, 72.0 (2×CH_2 of BnO), 70.8 (dd, $^2J_{C1,Fa}=33.7$ Hz, $^2J_{C1,Fb}=25.7$ Hz, C1), 65.7 ppm (C6); ^{19}F NMR (376 MHz, $CDCl_3$ $CFCl_3$, 298 K): $\delta=-100.8$ (brd, 1F, $^2J_{Fa,Fb}=257$ Hz, Fa), −106.2 ppm (brd, 1F, $^2J_{Fb,Fa}=256$ Hz, Fb); ESI QqTOF MS: calcd for ([*M*+Na]) 673.2742, found 673.2744; elemental analysis calcd (%) for $C_{41}H_{40}F_2O_5$: C 75.67, H 6.20; found: C 75.60, H 6.32.

2,6-Anhydro-1-deoxy-1,1-difluoro-3,4,5,7-tetra-*O*-benzyl-1-*C*-phenyl-D-*glycero*-L-*manno*-heptitol (12): In a PET vial containing the β-ketone **10** (0.040 g, 0.064 mmol), was added a solution of 50% Deoxo-Fluor in THF (0.60 mL, 0.62 g, 1.40 mmol) followed by two drops of HF-pyridine as the catalyst at 25°C under argon. The reaction mixture was heated to 50°C for 5 h, 60°C for 8 h, 65°C for 8 h, and 70°C for 8 h (in this way THF was evaporated slowly out of the reaction mixture). The reaction was quenched by pouring the mixture dropwise into a mixture of saturated aqueous $NaHCO_3$ and ice. It was allowed to reach 25°C and was then extracted with Et_2O (3×15 mL). The combined organic layers were washed with brine, dried over $MgSO_4$, and concentrated in vacuo. The residue was purified by FC (5% EtOAc in petroleum ether) to give **12** (0.009 g, 23%) as a yellowish oil (28% of starting material was also recovered). $[\alpha]_D^{25}=+12$ ($c=0.155$, $CHCl_3$); IR (neat): $\tilde{\nu}=1453$, 1406, 1394, 1380, 1250, 1075, 1066, 1057, 733, 696 cm^{-1}; ^1H NMR (400 MHz, $CDCl_3$, 298 K): $\delta=7.58$–7.60 (m, 2H), 7.24–7.39 (m, 21H), 7.15–7.18 (m, 2H) H_{arom}, 4.95 (d, 1H, $^2J=12.0$ Hz), 4.84 (d, 1H, $^2J=9.9$ Hz), 4.75 (d, 1H, $^2J=11.7$ Hz), 4.70 (d, 1H, $^2J=11.4$ Hz), 4.67 (d, 1H, $^2J=9.9$ Hz), 4.59 (d, 1H, $^2J=12.0$ Hz), 4.27 (brs, 2H) 4×CH_2 of BnO, 4.14 (dd, 1H, $^3J_{H2,H1}=9.6$ Hz, $^3J_{H2,H3}=9.2$ Hz, H2), 3.92 (d, 1H, $^3J_{H4,H3}=2.8$ Hz, H4), 3.86 (ddd, 1H, $^3J_{H1,Fb}=14.5$ Hz, $^3J_{H1,H2}=9.6$ Hz, $^3J_{H1,Fa}=5.5$ Hz, H1), 3.67 (dd, 1H, $^3J_{H3,H2}=9.2$ Hz, $^3J_{H3,H4}=2.8$ Hz, H3), 3.47–3.53 ppm (m, 3H, H5, H6a,b); ^{13}C NMR (100 MHz, $CDCl_3$, 298 K): $\delta=138.7$, 138.2, 138.1, 137.9 C_{ipso} of BnO, 135.4 (t, $^2J_{C,Fa}=^2J_{C,Fb}=25.7$ Hz, C_{ipso} of Ph), 129.7, 128.4, 128.32, 128.3, 128.2, 128.16, 127.9, 127.73, 127.68, 127.6, 127.56, 127.4 C_{arom} of BnO, 126.1 (t, $^3J_{C,Fa}=^3J_{C,Fb}=6.4$ Hz, C_{ortho} of Ph), 120.3 (t, $^1J_{C,Fa}=^1J_{C,Fb}=248$ Hz, CF_2), 84.5 (C3), 79.6 (t, $^2J_{C1,Fa}=^2J_{C1,Fb}=29.7$ Hz, C1), 77.4 (C5), 75.0 (CH_2 of BnO), 74.8 (C2), 74.1, 73.4 (2×CH_2 of BnO), 73.3 (C4), 72.6 (CH_2 of BnO), 68.9 (C6); ^{19}F NMR (376 MHz, $CDCl_3$ $CFCl_3$, 298 K): δ ppm −97.6 (dd, 1F, $^2J_{Fa,Fb}=257$ Hz, $^3J_{Fa,H1}=4.4$ Hz, Fa), −108.6 ppm (dd, 1F, $^2J_{Fb,Fa}=258$ Hz, $^3J_{Fb,H-1}=14.4$ Hz, Fb); ESI QqTOF MS: calcd for ([*M*+Na]) 673.2742, found 673.2739; elemental analysis calcd (%) for $C_{41}H_{40}F_2O_5$: C 75.67, H 6.20; found: C 75.60, H 6.34.

2,6-Anhydro-1-deoxy-1,1-difluoro-1-*C*-phenyl-D-*glycero*-L-*gluco*-heptitol (2): Pd/C 10% (0.80 g) under argon was added to a solution of the benzyl-protected difluoride **11** (0.372 g, 0.57 mmol) in EtOH (45 mL). Argon was exchanged by H_2 gas and the reaction mixture was stirred under an H_2 atmosphere (1 atm) at 25°C for 38 h. Then, it was filtered carefully through Celite and the filtrate was concentrated in vacuo. The residue was purified by FC (10% MeOH in CH_2Cl_2) to give **2** (0.116 g, 70%) as a colorless oil that solidified after drying and standing in the freezer. Some of the oil was recrystallized from *i*PrOH, affording colorless crystals of **2**. m.p. 128–130°C; $[\alpha]_D^{25}=+34$ ($c=0.085$, MeOH); IR (neat): $\tilde{\nu}=3345$, 2925, 2483 (br, OH), 1451, 1271, 1062, 1002, 971, 763, 700 cm^{-1}; ^1H NMR (400 MHz, CD_3OD, 298 K): $\delta=7.56$–7.59 (m, 2H, H_{ortho}), 7.42–7.45 (m, 3H, H_{meta}, H_{para}), 4.41 (ddd, 1H, $^3J_{H1,Fa}\approx^3J_{H1,Fb}\approx14.3$ Hz, $^3J_{H1,H2}=2.8$ Hz, H1), 4.16 (dd, 1H, $^3J_{H4,H5}=4.9$ Hz, $^3J_{H4,H3}=3.0$ Hz, H4), 3.99 (ddd, 1H, $^3J_{H5,H6a}=7.0$ Hz, $^3J_{H5,H4}\approx^3J_{H5,H6b}\approx4.6$ Hz, H5), 3.89 (dd, 1H, $^3J_{H3,H2}\approx6.6$ Hz, $^3J_{H3,H4}\approx3.4$ Hz, H3), 3.86 (dd, 1H, $^3J_{H2,H3}\approx6.5$ Hz, $^3J_{H2,H1}\approx3.2$ Hz, H2), 3.83 (dd, 1H, $^2J_{H6a,H6b}=12.0$ Hz, $^3J_{H6a,H5}=7.2$ Hz, H6a), 3.68 ppm (dd, 1H, $^2J_{H6b,H6a}=12.0$ Hz, $^3J_{H6b,H5}=4.2$ Hz, H6b); ^{13}C NMR (100 MHz, CD_3OD, 298 K): $\delta=137.5$ (t, $^2J_{C,Fa}=^2J_{C,Fb}=25.3$ Hz, C_{ipso}), 130.9 (C_{para}), 129.2 (C_{meta}), 126.7 (t, $^3J_{C,Fa}=^3J_{C,Fb}=6.8$ Hz, C_{ortho}), 123.3 (t, $^1J_{C,Fa}=^1J_{C,Fb}=249$ Hz, CF_2), 78.2 (C5), 73.6 (t, $^2J_{C1,Fa}=^2J_{C1,Fb}=27.3$ Hz, C1), 72.2 (C3), 69.9 (C2), 67.4 (C4), 60.3 ppm (C6); ^{19}F NMR (376 MHz, CD_3OD $CFCl_3$, 298 K): $\delta=-99.5$ (brd, 1F, $^2J_{Fa,Fb}=254$ Hz, F_a), −101.1 ppm (brdd, 1F, $^2J_{Fb,Fa}=254$ Hz, $^3J_{Fb,H1}\approx15.3$ Hz, F_b); ESI QqTOF MS: calcd for ([*M*+Na]) 313.0863, found 313.0866; elemental analysis calcd (%) for $C_{13}H_{16}F_2O_5$: C 53.79, H 5.56; found: C 53.79, H 5.54.

2,6-Anhydro-1-deoxy-1,1-difluoro-1-*C*-phenyl-D-*glycero*-L-*manno*-heptitol (3): Benzyl-protected difluoride **12** (0.021 g, 0.032 mmol) was submitted to hydrogenation under the conditions described above for the preparation of compound **2**. FC (10% MeOH in CH_2Cl_2) afforded **3** as a yellowish oil (0.006 g, 67%). $[\alpha]_D^{25}=-14$ ($c=0.07$, MeOH); IR (neat): $\tilde{\nu}=3661$, 3423 (br, OH), 1449, 1393, 1236, 1144, 1100, 1075, 1066, 1051, 983, 862, 760, 692 cm^{-1}; ^1H NMR (400 MHz, CD_3OD, 298 K): $\delta=7.55$–7.59 (m, 2H, H_{ortho}), 7.38–7.43 (m, 3H, H_{meta}, H_{para}), 3.87 (brd, 1H, $^3J_{H4,H3}=3.2$ Hz, H4), 3.57–3.74 (m, 4H, H1, H2, H6a,b), 3.44–3.51 ppm (m, 2H, H3, H5); ^{13}C NMR (100 MHz, CD_3OD, 298 K): $\delta=136.8$ (C_{ipso}), 130.8 (C_{para}), 128.9 (C_{meta}), 127.3 (t, $^3J_{C,Fa}=^3J_{C,Fb}=6.4$ Hz, C_{ortho}), 121.9 (t, $^1J_{C,Fa}=^1J_{C,Fb}=247$ Hz, CF_2), 81.5 (t, $^2J_{C1,Fa}=^2J_{C1,Fb}=29.0$ Hz, C1), 80.3 (C5), 76.2 (C3), 70.1 (C4), 68.4 (C2), 62.2 ppm (C6); ^{19}F NMR (376 MHz, CD_3OD $CFCl_3$, 298 K): $\delta=-96.4$ (brdd, 1F, $^2J_{Fa,Fb}=260$ Hz, $^3J_{Fa,H1}\approx4.9$ Hz, Fa), −105.9 ppm (brdd, 1F, $^2J_{Fb,Fa}=259$ Hz, $^3J_{Fb,H1}\approx12.0$ Hz, Fb); ESI QqTOF MS: calcd for ([*M*+Na]) 313.0863, found 313.0883; elemental analysis calcd (%) for $C_{13}H_{16}F_2O_5$: C 53.79, H 5.56; found: C 53.42, H 5.30.

Acknowledgements

Financial support by the Swiss National Science Foundation (Bern) is acknowledged by the Lausanne group. The group at Madrid thanks the Ministry of Science and Innovation of Spain for a research grant (CTQ2006-10874-C02—01) and the Munich group acknowledges generous support by the research initiative LMU*excellent* and an EC Marie Curie Research Training network (MRTN-CT-2005—019561). We also thank M. Rey, Dr. A. Razaname, A. Gillig, Dr. R. Scopelliti for technical help, and C. Flowers for revising the manuscript (EPFL).

[1] *The Sugar Code. Fundamentals of Glycosciences* (Ed.: H.-J. Gabius), Wiley-VCH, Weinheim, **2008**.

[2] a) D. Solís, J. Jiménez-Barbero, H. Kaltner, A. Romero, H.-C. Siebert, C.-W. von der Lieth, H.-J. Gabius, *Cells Tissues Organs* **2001**, *168*, 5–23; b) H.-J. Gabius, H.-C. Siebert, S. André, J. Jiménez-Barbero, H. Rüdiger, *ChemBioChem* **2004**, *5*, 740–764.
[3] a) H.-J. Gabius, *Biochimie* **2001**, *83*, 659–666; b) F. Stirpe, *Toxicon* **2004**, *44*, 371–383; c) M. Jiménez, J. L. Sáiz, S. André, H.-J. Gabius, D. Solís, *Glycobiology* **2005**, *15*, 1386–1395.
[4] a) S. André, Z. Pei, H.-C. Siebert, O. Ramström, H.-J. Gabius, *Bioorg. Med. Chem.* **2006**, *14*, 6314–6326; b) S. André, C. E. P. Maljaars, K. M. Halkes, H.-J. Gabius, J. P. Kamerling, *Bioorg. Med. Chem. Lett.* **2007**, *17*, 793–798.
[5] a) P. Sears, C.-H. Wong, *Angew. Chem.* **1999**, *111*, 2446–2471; *Angew. Chem. Int. Ed.* **1999**, *38*, 2300–2324; b) L. A. Marcaurelle, C. R. Bertozzi, *Chem. Eur. J.* **1999**, *5*, 1384–1390.
[6] a) J.-M. Beau, B. Vauzeilles, T. Skrydstrup in *Glycoscience: Chemistry and Chemical Biology, Vol. 3* (Eds.: B. Fraser-Reid, K. Tatsuta, J. Thiem), Springer, Berlin, **2001**, pp. 2679–2724; b) *Glycomimetics: Modern Synthetic Methodologies* (Ed.: R. Roy), ACS, Washington, **2005**; c) D. E. Levy in *The Organic Chemistry of Sugars* (Eds.: D. E. Levy, P. Fügedi), CRC, Boca Raton, **2006**, pp. 269–348.
[7] a) J. L. Asensio, F. J. Cañada, X. Cheng, N. Khan, D. R. Mootoo, J. Jiménez-Barbero, *Chem. Eur. J.* **2000**, *6*, 1035–1041; b) V. García-Aparicio, M. d. C. Fernández-Alonso, J. Angulo, J. L. Asensio, F. J. Cañada, J. Jiménez-Barbero, D. R. Mootoo, X. Cheng, *Tetrahedron: Asymmetry* **2005**, *16*, 519–527.
[8] a) M. S. Searle, D. H. Williams, *J. Am. Chem. Soc.* **1992**, *114*, 10690–10697; b) J. L. Asensio, J. F. Espinosa, H. Dietrich, F. J. Cañada, R. R. Schmidt, M. Martín-Lomas, S. André, H.-J. Gabius, J. Jiménez-Barbero, *J. Am. Chem. Soc.* **1999**, *121*, 8995–9000.
[9] J.-F. Espinosa, M. Bruix, O. Jarreton, T. Skrydstrup, J.-M. Beau, J. Jiménez-Barbero, *Chem. Eur. J.* **1999**, *5*, 442–448.
[10] a) B. E. Smart, *J. Fluorine Chem.* **2001**, *109*, 3–11; b) J. C. Biffinger, H. W. Kim, S. G. DiMagno, *ChemBioChem* **2004**, *5*, 622–627.
[11] a) M. J. Tozer, T. F. Herpin, *Tetrahedron* **1996**, *52*, 8619–8683; b) D. O'Hagan, H. S. Rzepa, *Chem. Commun.* **1997**, 645–652; c) H.-J. Böhm, D. Banner, S. Bendels, M. Kansy, B. Kuhn, K. Müller, U. Obst-Sander, M. Stahl, *ChemBioChem* **2004**, *5*, 637–643; d) Y. Xu, L. Qian, A. V. Pontsler, T. M. McIntyre, G. D. Prestwich, *Tetrahedron* **2004**, *60*, 43–49.
[12] a) N. C. Craig, A. Chen, K. H. Suh, S. Klee, G. C. Mellau, B. P. Winnewisser, M. Winnewisser, *J. Am. Chem. Soc.* **1997**, *119*, 4789–4790; b) C. R. S. Briggs, D. O'Hagan, H. S. Rzepa, A. M. Z. Slawin, *J. Fluorine Chem.* **2004**, *125*, 19–25.
[13] For CF_2-furanosides see: a) W. B. Motherwell, B. C. Ross, M. J. Tozer, *Synlett* **1989**, 68–70; b) J. S. Houlton, W. B. Motherwell, B. C. Ross, M. J. Tozer, D. J. Williams, A. M. Z. Slawin, *Tetrahedron* **1993**, *49*, 8087–8106; c) T. F. Herpin, W. B. Motherwell, M. J. Tozer, *Tetrahedron: Asymmetry* **1994**, *5*, 2269–2282; d) T. F. Herpin, W. B. Motherwell, J.-M. Weibel, *Chem. Commun.* **1997**, 923–924; e) J. Kovensky, D. Burrieza, V. Colliou, A. F. Cirelli, P. Sinaÿ, *J. Carbohydr. Chem.* **2000**, *19*, 1–12; f) H. Berber, T. Brigaud, O. Lefebvre, R. Plantier-Royon, C. Portella, *Chem. Eur. J.* **2001**, *7*, 903–909.
[14] For CF_2- and CHF-pyranosides see: a) S. Marcotte, F. D'Hooge, S. Ramadas, C. Feasson, X. Pannecoucke, J. C. Quirion, *Tetrahedron Lett.* **2001**, *42*, 5879–5882; b) J. Jiménez-Barbero, R. Demange, K. Schenk, P. Vogel, *J. Org. Chem.* **2001**, *66*, 5132–5138; c) A. B. Cuenca, F. D'Hooge, V. Gouge, G. Castelot-Deliencourt, H. Oulyadi, E. Leclerc, P. Jubault, X. Pannecoucke, J.-C. Quirion, *Synlett* **2005**, 2627–2630; d) A. Wegert, M. Hein, H. Reinke, N. Hoffmann, R. Miethchen, *Carbohydr. Res.* **2006**, *341*, 2641–2652; e) J. Picard, N. Lubin-Germain, J. Uzie, J. Auge, *Synthesis* **2006**, 979–982; f) N. P. Karche, C. Pierry, F. Poulain, H. Oulyadi, E. Leclerc, X. Pannecoucke, J.-C. Quirion, *Synlett* **2007**, 123–126; g) B. Moreno, C. Quehen, M. Rose-Hélène, E. Leclerc, J.-C. Quirion, *Org. Lett.* **2007**, *9*, 2477–2480; h) K. A. Tony, R. W. Denton, A. Dilhas, J. Jiménez-Barbero, D. R. Mootoo, *Org. Lett.* **2007**, *9*, 1441–1444; i) R. W. Denton, K. A. Tony, J. J. Hernández-Gay, F. J. Cañada, J. Jiménez-Barbero, D. R. Mootoo, *Carbohydr. Res.* **2007**, *342*, 1624–1635; j) G. Hirai, T. Watanabe, K. Yamaguchi, T. Miyagi, M. Sodeoka, *J. Am. Chem. Soc.* **2007**, *129*, 15420–15421; k) F. Poulain, A.-L. Serre, J. Lalot, E. Leclerc, J.-C. Quirion, *J. Org. Chem.* **2008**, *73*, 2435–2438.
[15] J. Pérez-Castells, J. J. Hernández-Gay, R. W. Denton, K. A. Tony, D. R. Mootoo, J. Jiménez-Barbero, *Org. Biomol. Chem.* **2007**, *5*, 1087–1092.
[16] a) R. R. Schmidt, H. Dietrich, *Angew. Chem.* **1991**, *103*, 1348–1349; *Angew. Chem. Int. Ed. Engl.* **1991**, *30*, 1328–1329; b) H. Dietrich, R. R. Schmidt, *Carbohydr. Res.* **1993**, *250*, 161–176; c) C. R. Johnson, B. A. Johns, *Synlett* **1997**, 1406–1408; d) P. Blom, B. Ruttens, S. Van Hoof, I. Hubrecht, J. van der Eycken, B. Sas, J. Van hemel, J. Vandenkerckhove, *J. Org. Chem.* **2005**, *70*, 10109–10112.
[17] Access to α-CF_2-galactosides was shown by Quirion and co-workers, see ref. [14a].
[18] a) O. E. Galanina, H. Kaltner, L. S. Khraltsova, N. V. Bovin, H.-J. Gabius, *J. Mol. Recognit.* **1997**, *10*, 139–147; b) M. Jiménez, S. André, H.-C. Siebert, H.-J. Gabius, D. Solís, *Glycobiology* **2006**, *16*, 926–937.
[19] For glycosyl carbaldehydes, see: a) W. R. Kobertz, C. R. Bertozzi, M. D. Bednarski, *Tetrahedron Lett.* **1992**, *33*, 737–740; b) A. Dondoni, M.-C. Scherrmann, *J. Org. Chem.* **1994**, *59*, 6404–6412; c) A. Dondoni, *Pure Appl. Chem.* **2000**, *72*, 1577–1588; d) A. Dondoni, A. Marra, *Chem. Rev.* **2004**, *104*, 2557–2599; e) J. Zeitouni, S. Norsikian, A. Lubineau, *Tetrahedron Lett.* **2004**, *45*, 7761–7763; f) G. Chen, M. Chien, M. Tsuji, R. W. Franck, *ChemBioChem* **2006**, *7*, 1017–1022.
[20] a) A. Giannis, K. Sandhoff, *Tetrahedron Lett.* **1985**, *26*, 1479–1482; b) L. Kröger, D. Henkensmeier, A. Schäfer, J. Thiem, *Bioorg. Med. Chem. Lett.* **2004**, *14*, 73–75.
[21] A. Dondoni, N. Catozzi, A. Marra, *J. Org. Chem.* **2005**, *70*, 9257–9268.
[22] A. Dondoni, N. Catozzi, A. Marra, *J. Org. Chem.* **2004**, *69*, 5023–5036.
[23] a) G. S. Lal, G. P. Pez, R. J. Pesaresi, F. M. Prozonic, H. Cheng, *J. Org. Chem.* **1999**, *64*, 7048–7054; b) R. P. Singh, J. M. Shreeve, *Synthesis* **2002**, 2561–2578.
[24] *NMR Spectroscopy of Glycoconjugates* (Eds.: J. Jiménez-Barbero, T. Peters), Wiley-VCH, Weinheim, **2002**.
[25] N. L. Allinger, Y. H. Yuh, J. H. Lii, *J. Am. Chem. Soc.* **1989**, *111*, 8551–8566.
[26] K. Bock, J. O. Duus, *J. Carbohydr. Chem.* **1994**, *13*, 513–543.
[27] D. Neuhaus, M. P. Williamson, *The Nuclear Overhauser Effect in Structural and Conformational Analysis*, Wiley-VCH, Weinheim, **1989**.
[28] J. L. Asensio, F. J. Cañada, A. García-Herrero, M. T. Murillo, A. Fernández-Mayoralas, B. A. Johns, J. Kozak, Z. Zhu, C. R. Jonson, J. Jiménez-Barbero, *J. Am. Chem. Soc.* **1999**, *121*, 11318–11329.
[29] A. Poveda, J. L. Asensio, M. Martín-Pastor, J. Jiménez-Barbero, *J. Biomol. NMR* **1997**, *10*, 29–43.
[30] M. Mayer, B. Meyer, *J. Am. Chem. Soc.* **2001**, *123*, 6108–6117.
[31] R. T. Lee, H.-J. Gabius, Y. C. Lee, *J. Biol. Chem.* **1992**, *267*, 23722–23727.
[32] J. L. Asensio, M. Martín-Pastor, J. Jiménez-Barbero, *Int. J. Biol. Macromol.* **1995**, *17*, 137–148.
[33] J. Jiménez-Barbero, J. F. Espinosa, J. L. Asensio, F. J. Cañada, A. Poveda, *Adv. Carbohydr. Chem. Biochem.* **2000**, *56*, 235–284.
[34] CCDC-683094 (**2**) contains the supplementary crystallographic data for this paper. These data can be obtained free of charge from The Cambridge Crystallographic Data Centre via www.ccdc.cam.ac.uk/data_request/cif
[35] J. Angulo, B. Langpap, A. Blume, T. Biet, B. Meyer, N. R. Krishna, H. Peters, M. M. Palcic, T. Peters, *J. Am. Chem. Soc.* **2006**, *128*, 13529–13538.
[36] Maestro, A powerful, all-purpose molecular modelling environment, Schrodinger LLC, **2005**.
[37] W. C. Still, A. Tempczyk, R. C. Hawley, T. Hendrickson, *J. Am. Chem. Soc.* **1990**, *112*, 6127–6129.
[38] J. W. Keepers, T. L. James, *J. Magn. Reson.* **1984**, *57*, 404–426.
[39] J. M. Alonso-Plaza, M. A. Canales, M. Jiménez, J. L. Roldán, A. García-Herrero, L. Iturrino, J. L. Asensio, F. J. Cañada, A. Romero,

H.-C. Siebert, S. André, D. Solís, H.-J. Gabius, J. Jiménez-Barbero, *Biochim. Biophys. Acta Gen. Subj.* **2001**, *1568*, 225–236.
[40] a) H.-J. Gabius, H. Walzel, S. S. Joshi, J. Kruip, S. Kojima, V. Gerke, H. Kratzin, S. Gabius, *Anticancer Res.* **1992**, *12*, 669–676; b) H.-J. Gabius, F. Darro, M. Remmelink, S. André, J. Kopitz, A. Danguy, S. Gabius, I. Salmon, R. Kiss, *Cancer Invest.* **2001**, *19*, 114–126; c) S. André, H. Kaltner, T. Furuike, S.-I. Nishimura, H.-J. Gabius, *Bioconjugate Chem.* **2004**, *15*, 87–98; d) J. C. Manning, K. Seyrek, H. Kaltner, S. André, F. Sinowatz, H.-J. Gabius, *Histol. Histopathol.* **2004**, *19*, 1043–1060; e) V. García-Aparicio, M. Sollogoub, Y. Blériot, V. Colliou, S. André, J. C. Asensio, F. J. Gañada, H.-J. Gabius, P. Sinaÿ, J. Jiménez-Berbero, *Carbohydr. Res.* **2007**, *342*, 1918–1928.
[41] For recent examples in the carbohydrate field, see: a) R. S. Houliston, N. Yuki, T. Hirama, N. H. Khieu, J.-R. Brisson, M. Gilbert, H. C. Jarrell, *Biochemistry* **2007**, *46*, 36–44; b) T. Haselhorst, H. Blanchard, M. Frank, M. J. Kraschnefski, M. J. Kiefel, A. J. Szyczew, J. C. Dyason, F. Fleming, G. Holloway, B. S. Coulson, M. von Itzstein, *Glycobiology* **2007**, *17*, 68–81.
[42] K. Stott, J. Stonehouse, J. Keeler, T.-L. Hwang, A. J. Shaka, *J. Am. Chem. Soc.* **1995**, *117*, 4199–4200.
[43] M. Jiménez, S. André, H.-C. Siebert, H.-J. Gabius, D. Solís, *Glycobiology* **2006**, *16*, 926–937.
[44] G. M. Morris, D. S. Goodsell, R. S. Halliday, R. Huey, W. E. Hart, R. K. Belew, A. J. Olson, *J. Comput. Chem.* **1998**, *19*, 1639–1662.

Received: July 9, 2008
Published online: February 2, 2009

